

# Recent Advances in the Pharmaceutical and Biomedical Applications of Cyclodextrin-Capped Gold Nanoparticles

Ahmed AH Abdellatif<sup>1,2,\*</sup>, Fatma Ahmed<sup>3,\*</sup>, Ahmed M Mohammed<sup>2</sup>, Mansour Alsharidah<sup>4</sup>, Amal Al-Subaiyel<sup>1</sup>, Waad A Samman<sup>5</sup>, Aisha A Alhaddad<sup>5</sup>, Samiah Hamad Al-Mijalli<sup>6</sup>, Mohammed A Amin<sup>1,2</sup>, Hassan Barakat<sup>7,8</sup>, Shaaban K Osman<sup>2,\*</sup>

<sup>1</sup>Department of Pharmaceutics, College of Pharmacy, Qassim University, Qassim, 51452, Saudi Arabia; <sup>2</sup>Department of Pharmaceutics and Pharmaceutical Technology, Faculty of Pharmacy, Al-Azhar University, Assiut, 71524, Egypt; <sup>3</sup>Department of Zoology, Faculty of Science, Sohag University, Sohag, 82524, Egypt; <sup>4</sup>Department of Physiology, College of Medicine, Qassim University, Buraydah, 51452, Saudi Arabia; <sup>5</sup>Department of Pharmacology and Toxicology, College of Pharmacy, Taibah University, Medina, 42353, Saudi Arabia; <sup>6</sup>Department of Biology, College of Sciences, Princess Nourah Bint Abdulrahman University, Riyadh, 11671, Saudi Arabia; <sup>7</sup>Department of Food Science and Human Nutrition, College of Agriculture and Veterinary Medicine, Qassim University, Buraydah, 51452, Saudi Arabia; <sup>8</sup>Food Technology Department, Faculty of Agriculture, Benha University, Moshtohor, 13736, Egypt

\*These authors contributed equally to this work

Correspondence: Shaaban KOsman, Department of Pharmaceutics and Pharmaceutical Technology, Faculty of Pharmacy, Al-Azhar University, Assiut, 71524, Egypt, Tel +2 01 129059936, Fax +2-088-312191, Email Shaabanosman@azhar.edu.eg; Ahmed AH Abdellatif, Department of Pharmaceutics, College of Pharmacy, Qassim University, Qassim, 51452, Saudi Arabia, Email a.abdellatif@qu.edu.sa

**Abstract:** The real problem in pharmaceutical preparation is drugs' poor aqueous solubility, low permeability through biological membranes, and short biological  $t_{1/2}$ . Conventional drug delivery systems are not able to overcome these problems. However, cyclodextrins (CDs) and their derivatives can solve these challenges. This article aims to summarize and review the history, properties, and different applications of cyclodextrins, especially the ability of inclusion complex formation. It also refers to the effects of cyclodextrin on drug solubility, bioavailability, and stability. Moreover, it focuses on preparing and applying gold nanoparticles (AuNPs) as novel drug delivery systems. It also studies the uses and effects of cyclodextrins in this field as novel drug carriers and targeting devices. The system formulated from AuNPs linked with CD molecules combines the advantages of both CD and AuNPs. Cyclodextrins benefit in increasing aqueous drug solubility, loading capacity, stability, and size control of gold NPs. Also, AuNPs are applied as diagnostic and therapeutic agents because of their unique chemical properties. Plus, AuNPs possess several advantages such as ease of detection, targeted and selective drug delivery, greater surface area, high loading efficiency, and higher stability than microparticles. In the present article, we tried to present the potential pharmaceutical applications of CD-derived AuNPs in biomedical applications including antibacterial, anticancer, gene-drug delivery, and various targeted drug delivery applications. Also, the article highlighted the role of CDs in the preparation and improvement of catalytic enzymes, the formation of self-assembling molecular print boards, the fabrication of supramolecular functionalized electrodes, and biosensors formation.

**Keywords:** AuNPs, nanotechnology, drug delivery, drug targeting, inclusion complexes, cancer management

## Introduction

Cyclodextrin (CD) and cyclic oligosaccharides, which combine glucose units (six units or more), are linked to each other by  $\alpha$ -1,4-glycosidic linkage forming a hollow truncated cone shape structure. It was isolated and first described by Villiers from a culture medium of *Bacillus Amylobacter*, which was grown in starch.<sup>1,2</sup> There are three famous kinds of cyclodextrins named alpha-cyclodextrin ( $\alpha$ -CD) containing six glucose molecules, beta-cyclodextrin ( $\beta$ -CD) of seven glucose molecules, and gamma-cyclodextrin ( $\gamma$ -CD) composed of eight glucose units (Figure 1A-C).<sup>3,4</sup> These three major CDs are non-hygroscopic and crystalline materials.<sup>5</sup> The important characteristics of the mentioned cyclodextrins are stated in Table 1. In addition, Figures 1D illustrate the chemical structures of different CDs. Based on their architecture,

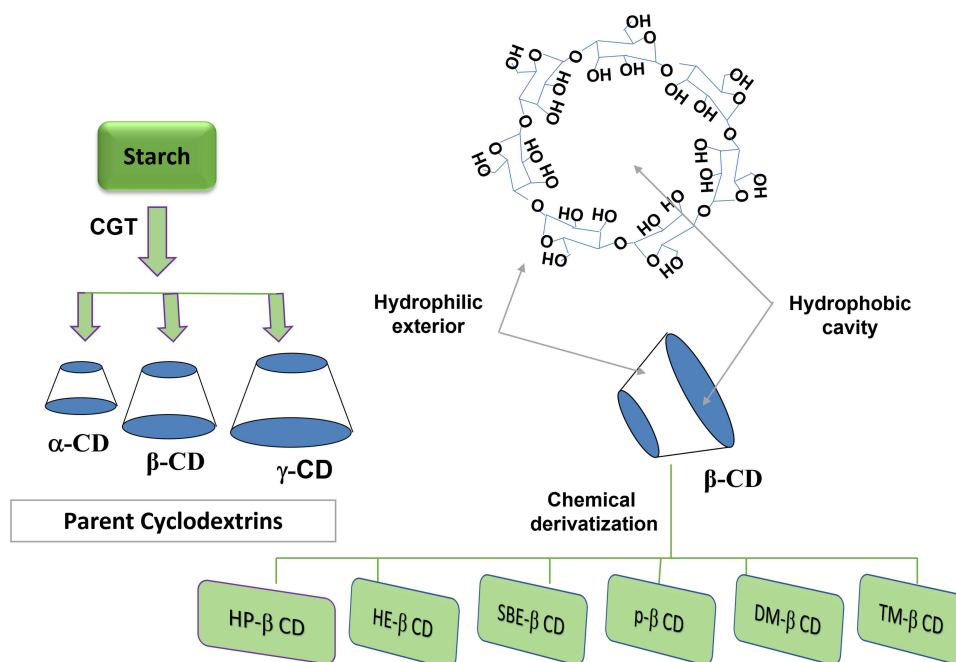


**Figure 1** Schematic representation of  $\alpha$ -,  $\beta$ -, and  $\gamma$ -Cyclodextrin, and the chemical derivatization of  $\beta$ -CD molecule.

toroidal or cone-shaped, there are two open-sided (one narrow side and the other is wider). The hydroxyl groups are in the periphery and classified into two categories, primary and secondary hydroxyl groups. The secondary OH groups are located on the wider edges of cyclodextrin molecules. The primary (-OH) groups are located on the narrow side of the CD torus. The melting points of  $\alpha$ -,  $\beta$ -, and  $\gamma$ -CD are between 240°C and 265°C.<sup>6,7</sup>

The aqueous solubility of  $\beta$ -CD is lower than that of the linear dextrin, which may be attributed to the strong internal hydrogen binding of the cyclodextrin molecules in its crystal state.<sup>10</sup> Chemical modifications were applied to produce highly water-soluble amorphous  $\beta$ -CD derivatives, including hydroxypropyl- $\beta$ -CD, sulfobutylether- $\beta$ -CD, and epichlorohydrin- $\beta$ -CD polymer (more than 500 mg/mL) (Table 2).<sup>11,12</sup> Especially, the water-soluble polymerized  $\beta$ -CDs of higher molecular weight offer the advantages of complexation without toxic effects and amorphous state.<sup>13,14</sup>

Herein, we report on a new review, summarizing the recent advance in constructing CD-based gold nanoparticles (CD-AuNPs) functional systems. The present review article discusses design methodologies, physicochemical properties,

**Table 1** Distinctive Characteristic Features of  $\alpha$ -,  $\beta$ -, and  $\gamma$ -CDs.

Character	$\alpha$ -CD	$\beta$ -CD	$\gamma$ -CD
Glucose units	6	7	8
Mol. weight (Da)	972	1135	1297
Aqueous solubility (mg/mL)	145	18.5	232
Cavity diameter, nm	0.5	0.62	0.83
Height of the torus, nm	0.78	0.78	0.78
Outer periphery diameter, nm	1.46	1.54	1.75
The volume of the cavity, Å <sup>3</sup>	174	262	427
pK (by potentiometry) at 25°C	12.33	12.2	12.08

**Note:** Data from references.<sup>8,9</sup>

**Table 2** Characteristics of Different  $\beta$ -CD Derivatives

Character	$\beta$ -CD	HP- $\beta$ -CD	SBE- $\beta$ -CD	Methyl- $\beta$ -CD	p $\beta$ -CD
Molecular weight (kDa)	1.135	1.400	2.163	1.312	96–112
Aqueous solubility (mg/mL)	18.5	>600	>500	>500	>500

**Abbreviations:**  $\beta$ -CD,  $\beta$ -Cyclodextrin; HP- $\beta$ -CD, hydroxypropyl-beta-cyclodextrin, SBE- $\beta$ -CD, sulfobutylether-beta-cyclodextrin; methyl- $\beta$ -CD, methylated-beta-cyclodextrin; p $\beta$ -CD, polymerized-beta-cyclodextrin.

and unique advantages of different CD-based nanoparticles in detail. Also, the applications of the modified systems, including drug delivery, enzymatic catalysis, biomedical diagnosis, and sensing were highlighted in this article.

## Ability of Cyclodextrin to Form Inclusion Complexes

Cyclodextrins have relatively hydrophobic inner cavities and a hydrophilic outer surface covered with hydroxyl groups.<sup>8,15</sup> Therefore, CDs can provide a favorable environment for the inclusion of complex formation with hydrophobic organic bioactive compounds in different drug:CD ratios (1:1, 1:2, or 2:1).<sup>16,17</sup>

The phase solubility diagram will be useful for studying the inclusion complexation, which investigates the impact of CD (as a solubilizing agent) on the included drugs.<sup>18,19</sup> The investigated drugs' solubility behavior is classified, including category (A) and category (B) curves. The category (A) curves represent the soluble inclusion complexes formation, while the category (B)-type curves indicate the construction of poorly soluble inclusion complexes (Figure 2).<sup>18</sup> Also, the A-category curves are subclassified into different subtypes, including  $A_L$  (linearly, the guest solubility increases with the increase in CD concentration),  $A_P$  in which a positive deviation isotherm was obtained, and  $A_N$  (showing a negative deviation isotherm) subtypes.

Similarly, B types are subclassified into  $B_1$  and  $B_s$  subtypes, indicating the formation of insoluble inclusion complexes and partially soluble complexes, respectively.<sup>20</sup> The most famous, frequent, and simple drug: CD ratio is 1:1. However, experimentally, there are different other uncommon drugs: CD ratios such as 1:2, 2:1, 1:3, or even more complicated associations were reported.<sup>21,22</sup> The stoichiometric ratio ( $n$ ) can be determined by isothermal titration calorimetry (ITC), which gives other parameters in addition to the complex ratio named the enthalpy, the entropy, and the binding constant, indicating the complexing affinity of the selected drug to the kind of cyclodextrin cavity. For example, adamantane molecules showed a (1:1) stoichiometric ratio with  $\beta$ -CD due to the perfect ball-like structure, size,

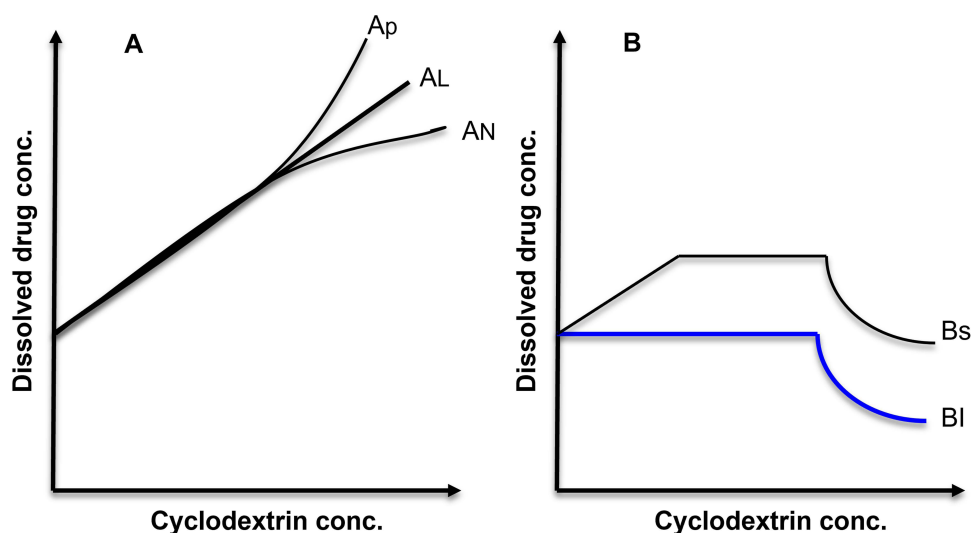


**Figure 2** Phase solubility diagram of  $\beta$ -CD. According to Higuchi and Connors, the types of phase-solubility diagrams of cyclodextrin presenting the solubility behavior of the included drugs upon increasing the CD concentration are two types (A and B) curves. Type (A) phase diagram is classified into three subtypes;  $A_L$ : linear diagram;  $A_P$ : positive deviation from linearity;  $A_N$ : negative deviation from linearity. Also, type (B) is classified into two subtypes;  $B_s$ : indicating the complex of limited solubility; and  $B_1$ : showing the insoluble complex.

and geometry of adamantane, which is suitable to form a perfect inclusion complex with  $\beta$ -CD. While as, in the case of cholesterol, as an example of larger molecules, the ITC results, which were reported previously indicated that the n value was (1:2) cholesterol: $\beta$ -CD. An equilibrium is established between the associated and the dissociated species upon dissolving or dissociating these complexes.<sup>23</sup> The obtained equilibrium of each complex is expressed by the stability constant (Ka).<sup>20,24</sup> For the 1:1 type of inclusion complexes, the equilibrium association or binding constant can be determined using the following equation.<sup>25</sup>

$$K_a = \text{slope}/S_0 (1-\text{slope}) \quad (1)$$

Where  $S_0$  is the intrinsic solubility of the drug. Also, the slope in the equation is the slope of the curve linear portion of solubility phase diagrams, which will be constructed by plotting the drug solubility against cyclodextrin concentration.

The formation of soluble inclusion complexes (solubilization properties) comes from the replacement of water molecules that exist in the hydrophobic cavities of cyclodextrin molecules by the hydrophobic guest molecules via hydrophobic–hydrophobic interaction.<sup>26,27</sup> Interestingly, the inclusion ability of CD molecules has been utilized as a base for their different pharmaceutical applications, including the solubility enhancement of hydrophobic drugs,<sup>28,29</sup> increasing their dissolution rate and bioavailability,<sup>30,31</sup> improving the guest stability and biological half-lives,<sup>32,33</sup> and even for several food industry applications.<sup>34</sup>

Moreover, the inclusion complexation ability of CDs was utilized as a base for the construction of more sophisticated supramolecular systems, including polymers,<sup>35,36</sup> hydrogels,<sup>37,38</sup> and nanoparticles.<sup>39,40</sup> Examples of previously reported inclusion complexes with CDs and their applications are displayed in Table 3.

It is worth mentioning that CD complexation usually involves a host: guest of 1:1 ratio; concurrently higher-order complicated complexations (2:1, 1:2, 2:2, etc) could occur. The complexation process takes place as the CD cavity is slightly non-polar in aqueous solutions; therefore, it could be entrapped via the non-covalent interaction by water molecules of high enthalpy that are ready to be replaced with other less polar “guest molecules” forming CD

**Table 3** Inclusion Complexes with Cyclodextrin and Their Applications

Year	Kind of CD	Drug	Formulation	Application	Ref.
2019	$\beta$ -CD	Basil and <i>Pimenta dioica</i> essential oils	Antimicrobial food preservation sachets	Improves thermal stability, decreases volatility, and increases the release duration of the essential oils	[27]
2016	$\beta$ -CD	Erlotinib	Nanosponge	Enhance solubility, dissolution rate, in vitro cytotoxicity, and oral bioavailability	[28]
2007	$\beta$ -CD and HP- $\beta$ -CD	5-fluorouracil	Thermosensitive mucoadhesive vaginal gel	Increases the drug aqueous solubility and release rate	[29]
2009	HP- $\beta$ -CD	Cisplatin	Solid inclusion complex		[41]
2016	$\beta$ -CD	Curcumin	Solid dispersion	Enhanced drug delivery and improved its therapeutic efficacy	[42]
2018	$\beta$ -CD, SBE- $\beta$ -CD, and HP- $\beta$ -CD	Amlodipine Limonin	Ophthalmic preparation	Improved ocular permeation and effectiveness of drug	[43]
2018	$\beta$ -CD and $\gamma$ -CD	Limonin Albendazole	Orange juice	Significant reduction of bitter taste and keep the anti-inflammatory effects of Limonin	[44]
2007	HP- $\beta$ -CD	Albendazole and Ricobendazole	Solid complex	Increase the drug solubility and efficacy with no signs of toxicity	[45]
2020	$\alpha$ -CD, $\beta$ -CD, and $\gamma$ -CD; and their derivatives (HP- $\beta$ -CD, and 2,6-di-O-methyl)- $\beta$ -CD (DM- $\beta$ -CD)	2R,3R-Dihydromyricetin flavonoid	1:1 stoichiometric inclusion complex	Enhanced the radical scavenging capacity of the drug and maintained its lipid-lowering effect (anti-hyperlipidemia)	[46]
2019	$\beta$ -CD	Tebipenem pivoxil	Solid inclusion complex	Improved drug chemical stability and antibacterial activity	[19]
2011	PM-CD, $\alpha$ -CD, $\beta$ -CD and $\gamma$ -CD, and HP- $\alpha$ -CD, HP- $\beta$ -CD and HP- $\gamma$ -CD	Lonidamine		Improved the solubility, bioavailability, and anticancer activity	[47]

complexes.<sup>48</sup> Noteworthy, several analytical techniques are applicable for characterizing the modified drug/CD complexes in the solid state, including thermo-analytical techniques (Differential scanning calorimetry (DSC), Thermogravimetric analysis (TGA), Hot-stage microscopy (HSM)), X-ray diffraction (Single crystal X-ray diffraction (SCXRD), powder X-ray diffraction (PXRD)), Spectroscopic techniques (Fourier-transform infra-red (FT-IR) spectroscopy, Attenuated total reflectance (ATR)-FTIR spectroscopy, and Raman spectroscopy), and Scanning electron microscopy (SEM).<sup>49</sup>

## Factors Affecting Inclusion Complex Formation

### Type and Cavity Size of Cyclodextrin

It was reported that the kind of CD molecules (native CDs or derivatives) affected both the formation and the effectiveness of guest/CD complexes. In the case of Ibuprofen, the increase in the drug dissolution rate has been obtained upon using either  $\beta$ - or  $\gamma$ -CD molecules, but  $\alpha$ -CD molecules were less suitable for stable inclusion complexes. The dissolution performance of the formed inclusion complexes appeared to be related to both the steric factors of the host molecule and the preparation method of the prepared solid systems. It was reported that the cavity size of  $\alpha$ -CD was less suitable for accommodating Ibuprofen as a guest molecule, whereas a true inclusion complex of such a drug in either  $\beta$ -CD or  $\gamma$ -CD cavities. The solubilizing efficiency of the drug enclosed within all investigated CDs was 8, 16, and 13 regarding  $\alpha$ -CD,  $\beta$ -CD, and  $\gamma$ -CD, respectively. Also, the stability constant of the formed complex was 65, 17,500, and 150, respectively.<sup>50</sup>

Also, better dissolution performance has been observed from the inclusion complexation of Ketoprofen with methyl-beta-cyclodextrin (M- $\beta$ CDs) compared to  $\beta$ -CDs.<sup>51</sup> Moreover, the polymerization of cyclodextrin improves the inclusion ability and accompanying characteristics of parent CDs since they were converted to the amorphous form.<sup>21</sup> Additionally, the formation of CD nano-sponges (CD-NS) was also accompanied by very high inclusion ability and encapsulation capacity.<sup>52,53</sup> Recently, the solubility and solution rate of docetaxel was affected by the CD type utilized in the inclusion complexation.<sup>54</sup>

### Drug Ionization State/Medium pH

The structure of both cyclodextrins (neutral as native CD or charged one as SBE-CD) and the guest molecules (positively or negatively charged) play an important role in the degree of inclusion complexation. Generally, the presence of charge on the cyclodextrin structure provides an additional site of interaction compared to neutral cyclodextrins. This may be attributed to the fact that the strength of inclusion complexation increased with the existence of opposite charge between the guest and the host due to the increase in electrostatic or ionic interaction.<sup>55</sup> In comparison with HP- $\beta$ -CD, SBE- $\beta$ -CD of negative charges increase the solubility and inclusion ability of positively charged drugs such as DY-9760e, a novel cytoprotective agent.<sup>56</sup> On the other hand, the ionization of the drug is an important issue in the complexation ability of native CDs (neutral). It was reported that the unionizable drugs are easier to form inclusion complexation with CDs than the ionizable ones. The value of K1:1 of non-ionized sulindac was 340 M<sup>-1</sup> at pH 2, and it was 139 M<sup>-1</sup> at pH 6.<sup>57</sup>

The complexation ability of CD molecules increases when the guest molecules carry opposite charges.<sup>56</sup> For example, the cationic (2-hydroxy-3-[tri-methyl-ammonia] propyl)- $\beta$ -CD acted as a very suitable solubilizer for many acidic drugs.<sup>58</sup> Also, the complexation of  $\beta$ -CD with a unionized form of sulindac was easier than in the case of an ionized one.<sup>57</sup> Regarding Piroxicam, the binding or stability constant values for the drug/CD complexes were affected by the change of pH values since it decreased by the increase in pH since it was 87 M<sup>-1</sup> and 29 M<sup>-1</sup> for pH 4.5 and 6, respectively. As a result, more effective complexation was obtained at an acidic pH.<sup>59</sup> Similarly, pH affects the thermodynamic stability of thymol and carvacrol inclusion complexes with  $\beta$ -CD in an aqueous medium.<sup>60</sup>

### Preparation Methods

Different techniques and methods were utilized for the preparation of inclusion complexes, including kneading (slurry),<sup>48,61,62</sup> solid dispersion,<sup>47,63</sup> grinding,<sup>64</sup> supercritical CO<sub>2</sub>,<sup>65</sup> microwave irradiation,<sup>66,67</sup> sealed heating,<sup>68</sup> freeze-

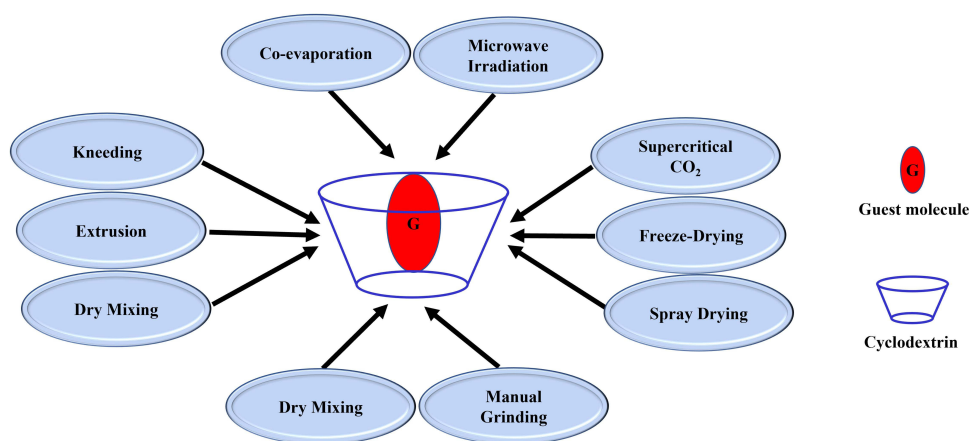


Figure 3 Schematic representation of the common CD complexation methods.

drying,<sup>69,70</sup> spray drying,<sup>71,72</sup> dry mixing,<sup>19</sup> damp (wet) mixing, extrusion, solvent evaporation, or co-precipitation.<sup>48</sup> Figure 3 and Table 4 summarize the common methods of CD complexation.

Noteworthy, the degree of complexation depends on the preparation method.<sup>23,113</sup> Both spray-drying and freeze-drying techniques were reported as the most effective drug/CD inclusion complexation methods. The enhanced

Table 4 Preparation Methods of CD Complexes

Year	Kind of CD	Drug	Method	Ref.
2007	β-CD	Reactive azo dyes	Dry Mixing (Dry Milling) (Ball Milling)	[73]
2016	β-CD	Ibuprofen		[74]
2019	β-CD	Tebipenem pivoxil		[19]
2001	β-CD	Ibuprofen	Kneading Damp Mixing (Wet Granulation)	[75]
2004	β-CD	Celecoxib (nonsteroidal anti-inflammatory drug)		[76]
2007	β-CD	Etoricoxib		[77]
2010	β-CD	Domperidone		[78]
2012	β-CD	Citronella oil & Citronellal & Citronellol		[79]
2004	β-CD & HP-β-CD	Quercetin	Freeze Drying (Lyophilization)	[80]
2005	β-CD	Scutellarin (in the presence of HP-Methylcellulose & Triethanolamine)		[81]
2018	HP-β-CD	Curcumin		[82]
2020	α-CD & β-CD & γ-CD; and their derivatives ((HP-β-CD & 2,6-di-O-methyl)-β-CD (DM-β-CD))	2R,3R-Dihydromyricetin (flavonoid)		[46]
2016	β-CD	Erlotinib		[28]
2007	β-CD & HP-β-CD	5-Fluorouracil		[29]
2009	HP-β-CD	Cisplatin		[41]
2010	β-CD & HP-β-CD	Flutamide (anticancer drug for prostatic carcinoma)		[83]
2011	HP-β-CD	Zerumbone		[84]
2012	β-CD	Oridonin		[70]

(Continued)

Table 4 (Continued).

Year	Kind of CD	Drug	Method	Ref.
2010	Methyl- $\beta$ -CD & HP- $\beta$ -CD & HP- $\gamma$ -CD	Exemestane (EXE) (irreversible aromatase inactivator)	Kneading & co-Lyophilization	[61]
2018	$\beta$ -CD	Black pepper oleoresin		[85]
2019	$\beta$ -CD	Basil & Pimenta dioica essential oils		[27]
2000	HP- $\beta$ -CD	Liposomes containing drugs alone or together: (Lecithin liposomes & entrapping Metronidazole & Verapamil)	Spray drying	[86]
2009	$\gamma$ -CD	Beclomethasone Dipropionate (corticosteroid)		[87]
2013	$\beta$ -CD	Quercetin		[88]
2017	HP- $\beta$ -CD & 2-O-M- $\beta$ -CD	Voriconazole		[89]
2017	Maltodextrin & $\gamma$ -CD	Pomegranate juice		[90]
2018	$\beta$ -CD	Chloramphenicol	Manual grinding	[91]
2002	$\beta$ -CD-EPI & $\beta$ -CD-EPS	Naproxen		[92]
2013	$\beta$ -CD	Rifaldazine		[93]
2013	HP- $\beta$ -CD	Rifampicin		[94]
2017	$\beta$ -CD & HP- $\beta$ -CD & RAMEB & SBE- $\beta$ -CD	Praziquantel	Grinding by high-energy vibrational mills	[95]
2016	$\beta$ CD & HP $\beta$ CD	Indomethacin nicotinamide cocrystals		[96]
2014	SBE- $\beta$ -CD + citric acid	Econazole nitrate		[97]
2018	$\beta$ -CD	Opipramol base	Grinding using planetary mills	[98]
2018	$\beta$ -CD & HP- $\beta$ -CD	Fluconazole	Extrusion	[99]
2019	HP- $\beta$ -CD	Carbamazepine printlets		[100]
2022	HP- $\beta$ -CD	Naringenin		[101]
2008	$\beta$ -CD	Piroxicam	Supercritical CO <sub>2</sub>	[102]
2013	Methyl- $\beta$ -CD	Ketoprofen		[103]
2007	$\beta$ -CD	Ibuprofen	Supercritical CO <sub>2</sub> techniques in comparison with other techniques	[104]
2007	$\beta$ -CD	Benzocaine		[105]
2007	$\beta$ -CD	Benzocaine & Bupivacaine & Mepivacaine (local anesthetic agents)		[106]
2008	$\beta$ -CD	Econazole		[107]
2009	$\beta$ -CD	Itraconazole & Econazole & Fluconazole (antifungal drugs)		[68]
2015	Methyl- $\beta$ -CD	Olanzapine		[108]
2019	$\beta$ -CD	Metformin hydrochloride		Microwave irradiation
2022	$\beta$ -CD	Edaravone	[67]	
2011	PM-CD & $\alpha$ -CD & $\beta$ -CD & $\gamma$ -CD & HP- $\alpha$ -CD & HP- $\beta$ -CD & HP- $\gamma$ -CD	Lonidamine	Solid dispersion	[47]
2016	$\alpha$ -CD & $\beta$ -CD & $\gamma$ -CD & HP- $\beta$ -CD	Etodolac (a preferential COX-2 inhibitor)		[109]
2019	$\beta$ -CD	Catechin		[63]

(Continued)

**Table 4** (Continued).

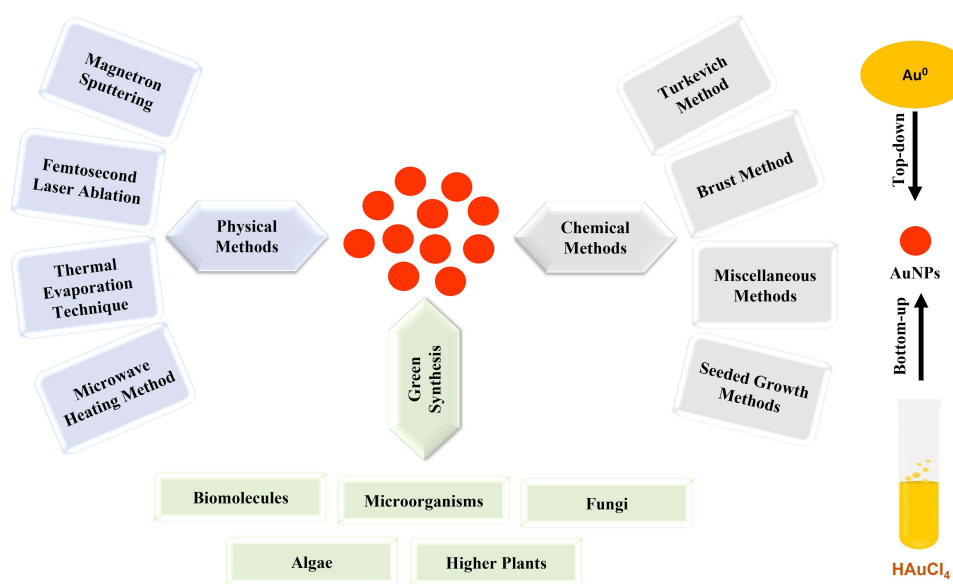
Year	Kind of CD	Drug	Method	Ref.
2018	HP- $\gamma$ -CD	Ibuprofen	Supercritical CO <sub>2</sub> -assisted Spray drying	[110]
2007	$\beta$ -CD	Albendazole & Ricobendazole	Co-evaporation(solvent evaporation)	[111]
2018	$\beta$ -CD & SBE- $\beta$ -CD & HP- $\beta$ -CD	Amlodipine Limonin		[43]
2005	$\beta$ -CD & HP- $\beta$ -CD	Ketoprofen	Co-evaporation & Sealed heating	[112]

dissolution rate of spray-dried products might be attributed to the decreased particle size, the high-energetic amorphous state, and the inclusion complex formation.<sup>114</sup> Also, as a powder production method commonly used in pharmaceutical fields, spray-drying possesses the advantages of being rapid, low-cost, and easily scalable. In addition, the spray-dried microcapsules were of spherical and uniform particle size. The solubility of the guest molecules upon using the spray-dried technique may be attributed to the encapsulation of the guest into the cylindrical cavity of cyclodextrin, and thus the thermal properties of the host and guest molecules were changed.<sup>115</sup>

## Gold Nanoparticles (AuNPs)

AuNPs are the most stable, fascinating, and attractive metal nanoparticles for nanotechnological research because of their stability, uniformity, biocompatibility, etc,<sup>17,116,117</sup> and also for their optical, electronic, magnetic, and supramolecular properties.<sup>118,119</sup> Additionally, AuNPs can conjugate many biological substances and form active complexes to provide targeted drug delivery.<sup>120</sup> Also, due to their very small size (nanoscales), AuNPs have a larger surface area. Consequently, the large surface area allowed better contact of AuNPs containing the bioactive molecules with the biological membranes and improved their bioavailability.<sup>17,20,121,122</sup> Regarding their application in medicine, AuNPs are utilized for the early detection and diagnosis of different diseases, as well as in their treatment.<sup>123,124</sup>

Stabilized noble metal NPs have been produced using one of the two main techniques, named bottom-up and top-down techniques (Figure 4). In the case of “top-down method” AuNPs can be produced from their constituent metals by the aid of microscopic machine and converted into nanoscale dimensions. Whereas in the bottom-up method, AuNPs can be produced from the gold atom solution using different methods as we will discuss below. There are three main methods

**Figure 4** Schematic representation of the common methods for AuNPs synthesis.

for AuNPs synthesis including chemical, physical, and biological methods.<sup>125</sup> In the chemical methods, the synthesis procedure involves the decomposition or precipitation of gold via the reduction of tetrachloro-auric acid ( $\text{HAuCl}_4$ ) as a gold precursor with the aid of a suitable reducing agent such as phosphorus,<sup>126</sup> citric acid,<sup>127</sup> sodium borohydride ( $\text{NaBH}_4$ ), or trisodium citrate.

The chemical procedure is the most famous and widely utilized technique because of its reagents' availability. This kind of the selected reducing agent affects the particle size of the produced colloids, which ranges from 1 to 100 nm.<sup>128</sup> For example, sodium citrate was utilized to produce AuNPs with a size range of 12–64 nm, depending upon the citrate/ $\text{HAuCl}_4$  ratio.<sup>127,129</sup> Also, the smaller particles (3–6 nm) are often prepared by using  $\text{NaBH}_4$  or a mixture of tannic acid and trisodium citrate.<sup>128,130</sup> The chemical method includes four main categories: Turkevich, Brust, Seeded growth, and Miscellaneous methods. The first two categories produce spherical AuNPs, while the other two categories generate various shaped (anisotropic) AuNPs (ie, rods, cubes, tubes, etc). Specifically, the Turkevich method includes the direct reduction of  $\text{Au}^{3+}$  ions into  $\text{Au}^0$  atoms using a reducing agent followed by stabilization using a stabilizing (capping) agent to generate a size range of 10–20 nm. Brust method includes the incorporation of the  $\text{Au}^{3+}$  ions into an organic solvent using a phase transfer agent (ie, Tetraoctylammonium Bromide (TOAB)) before the strong reduction using  $\text{NaBH}_4$  ( $\text{NaBH}_4$ ) to generate nanospheres of 1.5–5.2 nm. Seeded growth (anisotropic growth of AuNPs) is the most widely used technique that includes the strong reduction of the Au salt (ie, by using  $\text{NaBH}_4$ ) to form seed particles, which are then added to other metal salt solution (seed solution) in presence of a weak reducing agent (ie, ascorbic acid) + structure directing agent to generate various shaped AuNPs. Miscellaneous methods include ligands digestion using thiols, amines, silanes, phosphines, etc, or by ultrasonic waves, microwaves, laser ablation, solvothermal method, electrochemical, and photochemical reduction to generate mono-disperse AuNPs from poly-disperse AuNPs.<sup>125,131</sup>

Alternatively, different physical methods are utilized for the synthesis of anisotropic AuNPs.<sup>132</sup> One of these methods is the formation of gas-phase gold via thermal evaporation of gold under high vacuum. Then, the gas was allowed to be deposited on the surface of a single crystal substrate.<sup>133</sup> Another physical technique was utilized to produce gas-phase Au clusters via magnetron sputtering of a high-purity gold target with argon ions. To obtain uniformly dispersed AuNPs, the sputtered gold atoms were allowed to be deposited on the surface of a moving powder support material such as Aluminium Oxide ( $\gamma\text{-Al}_2\text{O}_3$ ). Separation of the loaded gold was achieved by using 5 mL of aqua regia (3:1 mixture of hydrochloric acid and nitric acid) that dissolved Au from the samples. Then,  $\gamma\text{-Al}_2\text{O}_3$  was separated and washed 3 times with deionized water.<sup>133,134</sup> Also, an ordered arrangement of AuNPs on an inclusion compound of  $\alpha\text{-CD}$ -dodecanethiol produced by magnetron sputtering. Here, a 2-D hexagonal lattice was formed from -SH groups of the guest molecule dodecanethiol linked with  $\alpha\text{-CD}$  interact with and stabilize AuNPs, which consequently arranged them in an ordered way.<sup>118</sup> Additionally, femtosecond laser ablation, an environmentally friendly alternative technique for producing monodispersed AuNPs, has also been proven since it can be applied at ambient conditions without any possible chemical contamination.<sup>135</sup> The advantages of physical techniques over other preparation methods include that the process is friendly to the environment since the excess gold can be recovered from the chamber. Moreover, no reducing agents have been utilized for the production. Hence, there is no solvent or precursor contamination.

Since physicochemical methods require and/or produce toxic byproducts of AuNPs, which are not suitable for biological applications, the recent trend is to modify AuNPs by using eco-friendly biological reagents for several bioapplications.<sup>136,137</sup> Green synthesis (Biosynthesis) of NPs is taking place using three main bio-strategies, including the use of biomolecules, microorganisms (bacteria and yeast), algae, fungi, and plant constituents<sup>138</sup> that are known to interact with the inorganic metals and could be used in bioleaching of minerals.<sup>131</sup> Table 5 displays certain studies on the common methods followed for the preparation of AuNPs.

Noteworthy, the properties (chemical, physical, or biological) of AuNPs are completely different compared with the corresponding gold ions. For example, we know that the color of bulk gold ions ( $\text{AuCl}_4$ ) is yellow. This color was changed from yellow to red upon the addition of a reducing agent such as sodium citrate with reflux, indicating the conversion of gold ions to NPs. Also, the color will be changed to dark grey-blue upon the addition of an excess reducing agent indicating the formation of aggregate or suspension of different sizes, dimensions, and plasmon resonance characteristics.<sup>162</sup> Besides, other properties can be affected by size and shape, including electromagnetic, optical, and

**Table 5** Different Preparation Methods Were Utilized for AuNPs Synthesis

Year	Method	Reagents	Comment	Ref.
<b>A. Physico-chemical techniques</b>				
<b>I. Chemical Methods</b>				
2007	Citrate Reduction (Turkevich methods)	<ul style="list-style-type: none"> <li>HAuCl<sub>4</sub> + Trisodium citrate (both the reducing agent and the stabilizer).</li> </ul>	Au <sup>3+</sup> was reduced to Au <sup>0</sup> by the oxidation of trisodium citrate to dicarboxylic acetone, then Au <sup>0</sup> atoms are formed when Au <sup>3+</sup> undergoes disproportionation.	[139]
2011			Monodisperse AuNPs (5–10 nm) were obtained.	[140]
2010		<ul style="list-style-type: none"> <li>Sodium citrate reducing agent + Solvent isotopic replacement (deuterium oxide for higher water replacement).</li> </ul>	Smaller sizes of AuNPs (5.3 ± 1.1 nm) were obtained in comparison with the diameter obtained in pure H <sub>2</sub> O (9.0 ± 1.2 nm).	[141]
2012		<ul style="list-style-type: none"> <li>Sodium citrate reducing agent + Altering the concentration of HAuCl<sub>4</sub></li> </ul>	Au NPs size range of 19–47 nm. Higher chloride ions decreased the surface charge and cause aggregates.	[130]
2012	Bitartrate Reduction (Turkevich methods)	<ul style="list-style-type: none"> <li>Potassium bitartrate-reducing agent</li> </ul>	Dark grey colloidal solution (not stable forming crystals), and dark red color by heating.	[142]
		<ul style="list-style-type: none"> <li>Potassium bitartrate reducing agent + a dispersion factor.</li> </ul>	Colloid gold with wine-red color (Polyethylene glycol dispersion factor), and dark purple-red color by heating (PVP dispersion factor).	
2003	Borohydride Reduction (Brust methods)	<ul style="list-style-type: none"> <li>Tetra-octyl-ammonium bromide (TOABr) (phase transfer reagent) + NaBH<sub>4</sub></li> </ul>	Monolayer protected AuNPs	[143]
2011	Borohydride Reduction (Miscellaneous methods)	<ul style="list-style-type: none"> <li>L-ascorbic acid (H<sub>2</sub>Asc) + NaBH<sub>4</sub> (NaBH<sub>4</sub>) (in presence of an alkanethiol).</li> <li>Polyvinyl alcohol (PVA) stabilizer.</li> </ul>	The smallest particles were 0.8–4 nm for the HAuCl <sub>4</sub> -H <sub>2</sub> Asc system and 0.6–3 nm for the HAuCl <sub>4</sub> -NaBH <sub>4</sub> system. Using polyvinyl alcohol (PVA) stabilizer produces stable colloids.	[144]
2007	(Seeded growth method)	<ul style="list-style-type: none"> <li>Seed solution: silver aqueous colloid solution (3–4 nm) stabilized by NaBH<sub>4</sub> and sodium citrate (reducing agent).</li> <li>Cetyltrimethylammonium bromide (CTAB), HAuCl<sub>4</sub>, and ascorbic acid + Seed solution.</li> </ul>	The nano-shape was controlled from rods to hollow spherical	[145]
2012	One-pot synthesis (Seeded growth method)	<ul style="list-style-type: none"> <li>CTAB (capping or structure directing agent) + ascorbic acid (reducing agent).</li> <li>AgNO<sub>3</sub> (nucleation and growth triggering agent).</li> </ul>	Anisotropic Au nanostars with multiple sharp spiky protrusions (The semimajor/semiminor axes of the two spheroids measured by SEM were 41/32 and 61/13 nm).	[146]
2011	One-pot synthesis (Seeded growth method)	<ul style="list-style-type: none"> <li>(AgNO<sub>3</sub> and CTAB) + (HAuCl<sub>4</sub>, and ascorbic acid)</li> </ul>	TEM measurements showed irregularly shaped small particles (30–50 nm) with protruded surfaces, after an initial stage of the reaction. After 5 min, particles become bigger in size (70–90 nm) with higher protrusions.	[147]
2002	Digestive ripening (Miscellaneous method)	<ul style="list-style-type: none"> <li>Dodecyltrimethylammonium bromide (DDAB) + toluene (Micelle solution).</li> <li>AuCl<sub>3</sub> + Micelle solution (surface-active ligand).</li> <li>Aqueous NaBH<sub>4</sub> (reducing agent) + AuCl<sub>3</sub>/Micelle solution.</li> </ul>	<ul style="list-style-type: none"> <li>Dark orange nanogold colloid turned red within 1 min.</li> <li>Polyhedral particle structure with reduced size and polydispersity (50 nm).</li> </ul>	[148]
<b>2. Physical methods</b>				
2005	One-step magnetron sputtering (By direct current of gold target)	<ul style="list-style-type: none"> <li>Dried high-surface-area γ-Al<sub>2</sub>O<sub>3</sub> (oxidation catalyst).</li> <li>Aqua regia for γ-Al<sub>2</sub>O<sub>3</sub> separation (3:1 mixture of hydrochloric acid and nitric acid)</li> <li>Deionized water (acids washing)</li> </ul>	<ul style="list-style-type: none"> <li>The most active size range (2–3 nm) was produced as measured by TEM.</li> </ul>	[134]
2007	Magnetron sputtering (By inclusion complexing)	<ul style="list-style-type: none"> <li>-α-cyclodextrin-dodecanethiol inclusion compound (stabilizing crystal plane).</li> </ul>	<ul style="list-style-type: none"> <li>2D hexagonal arrangement of particles (2–3 nm)</li> </ul>	[118]
2003	Femtosecond laser ablation	<ul style="list-style-type: none"> <li>Au metal plate + an aqueous solution of α-CD, β-CD, or γ-CD.</li> </ul>	<ul style="list-style-type: none"> <li>Stable AuNPs under the aerobic conditions without protective agents.</li> <li>A smaller size of ~2-2.4 nm with a narrow distribution of &lt;1–1.5 nm in correlation with the type and increase in the CD concentration.</li> </ul>	[135]
2019	One-step femtosecond-reactive laser ablation in liquid	<ul style="list-style-type: none"> <li>Directing pulses of a femtosecond laser beam on a silicon wafer immersed in an aqueous solution of KAuCl<sub>4</sub></li> <li>Porous silica (stabilizing agent).</li> </ul>	<ul style="list-style-type: none"> <li>Si reduced the particles size below 3 nm (more active size).</li> </ul>	[149]

(Continued)

Table 5 (Continued).

Year	Method	Reagents	Comment	Ref.
2008	Thermal evaporation technique	<ul style="list-style-type: none"> <li>• A substrate of multiwalled carbon nanotubes modified with Au nanoparticles by thermal evaporation.</li> </ul>	<ul style="list-style-type: none"> <li>• The size of the resulting hybrid structures on the carbon nanotubes influenced by the deposited Au film thickness.</li> <li>• The size ranged from 4 nm (spherical) to 150 nm (long wire-like).</li> <li>• The extent of Au depositions was increased by increasing the temperature</li> </ul>	[150]
2013		<ul style="list-style-type: none"> <li>• Glass substrates</li> <li>• electron-beam</li> <li>• Evaporation at substrate temperature of 250°C and deposition rate of 0.1–0.2 nm/s.</li> </ul>	<ul style="list-style-type: none"> <li>• Polycrystalline AuNPs had a size range of 14 and 19 nm</li> <li>• Increasing of mass thickness increased the particle size.</li> </ul>	[151]
2012	Microwave Heating method	<ul style="list-style-type: none"> <li>• <math>\beta</math>-CD, HAuCl<sub>4</sub>, NaOH</li> <li>• irradiation with 600W for 30 sec.</li> </ul>	<ul style="list-style-type: none"> <li>• The particle size of <math>\beta</math>-CD-AuNPs 20.6 nm and zeta potential -31mV.</li> </ul>	[152]
2021		<ul style="list-style-type: none"> <li>• <math>\beta</math>-CD, HAuCl<sub>4</sub>, NaOH</li> <li>• irradiation with 800W for 1 min.</li> </ul>	<ul style="list-style-type: none"> <li>• <math>\beta</math>-CD-AuNPs with particle size of 26.6 nm and zeta potential -22.7mV</li> </ul>	[153]
<b>B. Biological Methods (Green Synthesis)</b>				
2009	From biomolecules	<ul style="list-style-type: none"> <li>• Natural Honey</li> <li>• HAuCl<sub>4</sub> solution.</li> <li>• At room temperature.</li> </ul>	<ul style="list-style-type: none"> <li>• Spherical AuNPs of 15 nm size with high crystallinity.</li> </ul>	[154]
2018	From microorganisms (Bacteria)	<ul style="list-style-type: none"> <li>• Extract of the marine bacterium <i>Lysinibacillus odysey</i></li> <li>• Different temperature, pH, and HAuCl<sub>4</sub> concentration.</li> </ul>	<ul style="list-style-type: none"> <li>• Spherical AuNPs were obtained with a size range of 1–10 nm (average particle size = 5.6 ± 0.7 nm)</li> </ul>	[155]
2016	From microorganisms (Yeast)	<ul style="list-style-type: none"> <li>• <i>Magnusiomyces ingens</i> LH-F1</li> <li>• HAuCl<sub>4</sub> solution.</li> </ul>	<ul style="list-style-type: none"> <li>• AuNPs mixture of different shapes (spherical, plates, irregular) were obtained.</li> <li>• The average size reported 80.1 ± 9.8 nm by TEM and SEM.</li> <li>• DLS showed that the average size was 137.8 ± 4.6 nm.</li> </ul>	[156]
2018	From Fungi	<ul style="list-style-type: none"> <li>• -29 thermophilic filamentous fungi (reducing agents).</li> <li>• Comparing the extracellular extracts, the autolysates, or the intracellular fractions.</li> </ul>	<ul style="list-style-type: none"> <li>• Variable sized AuNPs (6–40 nm) were obtained depending on the used fungal strain and experimental conditions.</li> </ul>	[157]
2016	From algae	<ul style="list-style-type: none"> <li>• Aqueous extracts of two marine brown algae <i>Turbinaria conoides</i> and <i>Sargassum tenerrimum</i> (reducing and capping agent).</li> </ul>	<ul style="list-style-type: none"> <li>• Spherical AuNPs having an average size range of 27–35 nm.</li> </ul>	[158]
2018		<ul style="list-style-type: none"> <li>• The marine alga <i>Egria sp.</i> acted as reducing agent and as the stabilizing capping shell</li> </ul>	<ul style="list-style-type: none"> <li>• Spherical AuNPs having an average size range of 8–20 nm.</li> </ul>	[159]
2015	From higher plants	<ul style="list-style-type: none"> <li>• <i>Stevia rebaudiana</i> (SR) leaves extract</li> </ul>	<ul style="list-style-type: none"> <li>• Spherical AuNPs size range of from 5 to 20 nm.</li> </ul>	[160]
2019		<ul style="list-style-type: none"> <li>• <i>Olea europaea</i> fruit extract and <i>Acacia nilotica</i> husk extract</li> </ul>	<ul style="list-style-type: none"> <li>• The average size is 44.96 nm.</li> </ul>	[161]

catalytic properties.<sup>163</sup> Accordingly, the scientists were motivated to do their best to create a novel synthesis route that allows better size and shape control.

The surface plasmon resonance (SPR), the electron oscillation caused by electromagnetic radiation of the gold metal influences the photochemical characteristics of AuNPs, including the light scattering/absorption, photochemical conversion, and the enhancements of the electric field. The SPR depends basically on the AuNPs' geometries. The spherical NPs have one SPR value (520 nm). Also, it was reported that upon changing the diameter of NPs from 10 to 100 nm, it was found that the SPR value was shifted by 50 nm.<sup>164</sup> Also, SPR values were influenced markedly by changing the shape of the synthesized NPs, since the gold nanorods have two SPR values, depending on the electron oscillation along with two different directions. It was 520 nm in the transverse SPR since the oscillation occurs along the short axis. While the value ranged from (600–1100) nm, in longitudinal SPR (ie the oscillation of electrons takes place along the long axis).<sup>165</sup>

## Impact of $\beta$ -CD on AuNPs Properties and Applications

Several AuNPs, capped with thiolated CDs, were reported by different groups.<sup>166,167</sup> Most of these reports discussed the construction and characterization of CD-AuNPs. However, the safety and efficacy of NPs have limited entrapment



**Figure 5** Schematic representation of CD-AuNPs applications.

efficiency (with classical water emulsion polymerization procedures) which, consequently, requires the excessive administration of polymeric material.<sup>168</sup>

Herein, our review article discusses the incorporation of  $\beta$ -CD in AuNPs and highlights its applications in different pharmaceutical and biomedical fields. Generally, several applications of CDs (as illustrated in Figure 5) have been found attractive in the formulation of AuNPs, including the spontaneous formation, stabilization, and size control, the increase in loading capacity and bioavailability of the preparation, the improvement of catalytic enzymes, and the construction of functionalized electrodes, etc.<sup>15,169</sup>

## Stabilization and Size Controlling Role of CDs

It was reported that CD molecules have an important role in the control of nanoparticle size. For example, the size of CD-derived poly(isobutyl cyanoacrylate) nanospheres depends on CD type since the obtained NPs were 87 nm and 103 nm in the cases of HP- $\beta$ -CD or HP- $\gamma$ -CD, respectively. Furthermore, the concentration of the utilized CD can affect the size of the modified NPs. Upon increasing the concentration of HP- $\beta$ -CD from 0 to 12.5 mg/mL in the polymerization medium, the size of the modified NPs decreased from 300 to 50 nm. Also, it was noted that the values of zeta potential (Z-potential) of the modified particles decreased from -40 mV to 0 mV.<sup>170</sup> Noteworthy, the reduction of the value of the Z-potential is detrimental for the suspension since at low values of Z-potential the suspension becomes unstable, and the flocculation occurs.

Regarding the stabilization of the modified NPs, it was reported that CD molecules act as a steric stabilizer during the polymerization process of poly(isobutyl cyanoacrylate) in an aqueous medium.<sup>169</sup>

Cyclodextrin molecules bind directly to the surface of AuNPs via SH groups, and the AuNPs support the monolayer assembly of CDs.<sup>171</sup> The modified AuNPs can be affected by the type and concentration of the employed CD. The

smallest particles were obtained using gamma-CD ( $\gamma$ -SH-CD), followed by both  $\beta$ -SH-CD and  $\alpha$ -SH-CD. Also, the increase in the CD/AuCl<sub>4</sub> ratio was accompanied by a decrease in NPs particle size. CD-modified AuNPs were constructed directly by adding either Per-6-thio- $\beta$ -CD,<sup>166</sup> or Mono-6-lipoyl-amido-2,3,6-*O*-per methyl- $\beta$ -CD<sup>172</sup> to AuNPs solutions. The role of CDs in these modified systems was to control the aggregation of particles via the inclusion complexes formation.<sup>173</sup> Similarly, the polymerized CD was utilized to conjugate AuNPs and reported by another research group.<sup>174,175</sup> Besides, native cyclodextrins have been used and described in the preparation and characterization of AuNPs to investigate their impact on the size distribution of AuNPs. It was noted that the presence of CDs significantly reduced the size of AuNPs. The size of AUNPs was reduced from 12–15 to 4–6 nm by increasing the CD concentration. In addition, the kind of CD molecule affected the size of NPs since it was observed that the size value was 5.4 nm, 4.8, and 4.3 upon using  $\beta$ -CD,  $\alpha$ -CD, and  $\gamma$ -CD, respectively.<sup>120</sup> Some common characteristic effects on the modified AuNPs by their coupling CDs are listed in Table 6.

## Enhancing the Loading Capacity and Bioavailability

Cyclodextrins can include and solubilize hydrophobic molecules. The conjugation of AuNPs with CD molecules helps increase the hydrophobic cavities available for loading the bioactive agents. Therefore, the increase in CD number conjugating AuNPs increased the loading capacity.<sup>170,178</sup> Adeli and his coworkers reported the surface conjugation of gold NPs carriers with cyclodextrins/PEG poly-rotaxane, as a hybrid nano-system for improving solubility, bioavailability, and decreasing non-specific uptake of anticancer drugs (cisplatin and doxorubicin).<sup>176</sup> The modified CD nano-system allowed the controlled and targeted release of anticancer drugs, the enhanced permeability and the retention effect of both drugs, which were conjugated to AuNPs-hybrid nano-systems, which were endocytosed by cancer cells and, consequently, allowing the internally controlled drug release.<sup>176</sup>

In addition, the attachment of polyrotaxanes on the surface of AuNPs increased the internalization capacity of the modified system and anticancer drugs into the cells.<sup>176,179,180</sup> The modified new system composed of AuNPs core and polyrotaxane shell has dual advantages regarding the delivery of anticancer drugs. The nano-system can cross the cell membranes rapidly and decrease the anticancer's adverse effects. Also, the system comprising AuNPs can kill cancer cells via their photothermal properties.

Similarly, the inclusion ability of CD-coated AuNPs was utilized to construct a cytotoxic nano-drug system.<sup>178</sup> The idea was achieved via the inclusion complexation between  $\beta$ -CD and adamantane, end-capping oxo-platin (a prodrug of cisplatin). The results showed that the modified system still has anticancer efficiency with higher stability compared with free drugs.

Sierpe and his coworkers reported a ternary nano-system formulated by mixing AuNPs solution with the solution of a  $\beta$ -CD-loaded psychoactive drug (phenylethylamine). Full characterization of the constructed nanosystem was carried

**Table 6** Effect of CD on AuNPs Characteristics

Year	Kind of CD	Methods	Size characteristic	Ref.
2000	Perthiolated CDs ( $\alpha$ -, $\beta$ -, or $\gamma$ -)	<ul style="list-style-type: none"> <li>Reduction with NaBH<sub>4</sub> in DMSO containing Perthiolated CDs</li> </ul>	<ul style="list-style-type: none"> <li>Water-soluble, monolayer-coated gold colloids (or clusters) of spherical AuNPs (2–7 nm) in diameter.</li> </ul>	[173]
2003	Aqueous solution of $\alpha$ -CD, $\beta$ -CD, or $\gamma$ -CD.	<ul style="list-style-type: none"> <li>Femtosecond Laser Ablation</li> </ul>	<ul style="list-style-type: none"> <li>Particles size range of ~2-2.4 nm with narrow distribution of &lt;1–1.5 nm controlled by the type and concentration of CD.</li> </ul>	[135]
2003	$\alpha$ -CD, $\beta$ -CD, and $\gamma$ -CD	<ul style="list-style-type: none"> <li>Reduction with sodium citrate and NaBH<sub>4</sub></li> </ul>	<ul style="list-style-type: none"> <li>Decrease in size range was achieved by higher CD concentration as well as by NaBH<sub>4</sub> reduction.</li> </ul>	[120]
2011	$\beta$ -CD/Pluronic	<ul style="list-style-type: none"> <li>Citrate reduction</li> </ul>	<ul style="list-style-type: none"> <li>CD decreases the hydrodynamic size distribution of the nanosystem, which increases the loading capacity of Doxorubicin.</li> </ul>	[176]
2021	<ul style="list-style-type: none"> <li>Polymeric cationic CD (PolyCD) grafted on graphene layers (reducing and capping agents)</li> <li>Bisadamantane</li> <li>HAuCl<sub>4</sub></li> </ul>	<ul style="list-style-type: none"> <li>Direct reduction on the graphene surface.</li> </ul>	<ul style="list-style-type: none"> <li>PolyCD@BisAda@GCD/Au nano-assembly was obtained with a size range of 134 ± 53 nm.</li> <li>PolyCD@BisAda induced the formation of AuNPs that were not formed using graphene alone.</li> </ul>	[175]
2022	<ul style="list-style-type: none"> <li><math>\alpha</math>-CD</li> <li><math>\beta</math>-CD</li> </ul>	<ul style="list-style-type: none"> <li>Chemical reduction with o-hydroxybenzoic acid.</li> </ul>	<ul style="list-style-type: none"> <li>Stabilization with <math>\alpha</math>-CD and <math>\beta</math>-CD reduced the size of AuNPs as detected by DLS.</li> </ul>	[177]

out, and the results showed that the modified system would allow the release of the loaded drug after photothermal laser irradiation.<sup>181</sup>

Park and his coworkers reported a new nano-assembly that was constructed from the coating of AuNPs with CDs (AuNP/CD). The modified system was utilized to load or encapsulate an anticancer drug called  $\beta$ -Lapachone.<sup>182</sup> Besides, the incorporation of CDs in the gold nano-system was utilized as host cavities for the inclusion of targeting moieties called anti-epidermal growth factor (Anti-EGFR) receptor antibodies. There are two kinds of cancer cell lines, MCF-7 and A549. The results showed that the intercellular uptake and the extent of cellular inhibition of AuNPs-loaded drug were higher in the case of the system containing the targeting ligand than that does not contain the targeting ligand.<sup>182</sup>

Gimenez and his co-workers report the modification of AuNPs by SH- $\beta$ -CD. The modified nano-system was utilized to incorporate violacein as an anticancer agent via inclusion complexation with CD cavities to improve its solubility and bioavailability. The results illustrated that the loaded drug exhibited higher cytotoxic potential (based on MTT assay) on human leukemia cells (HL60) and lung fibroblast cells (V79) in comparison with the free drug.<sup>183</sup> Table 7 lists the role of CD complexation in enhancing the characteristics of the loaded bioactive molecules.

## Role of CD-AuNPs in Drug Targeting/Delivery

The presence of hydrophobic cavities in the CD structure makes it possible to carry certain hydrophobic materials or bioactive agents.<sup>184</sup> CDs and their derivatives, formed via structural modification of either primary or secondary face of parent CDs with aliphatic hydrocarbon chains, have been considered as potential excipients for different applications, including the production of nanospheres or nano-capsules of high loading capacity providing efficient targeting delivery.<sup>185,186</sup>  $\beta$ -CD derived nanoparticles were reported for loading and release of Tamoxifen.<sup>184</sup> The results indicated that the drug was either included in CD cavities or entangled in the aliphatic chains, allowing the release of the drug in a controlled-release manner.<sup>184</sup> However, the application of  $\beta$ -CD as a drug carrier is restricted by its low aqueous solubility, which could be enhanced by structural modification of the parent CD and the design of new formulations such as formulations of  $\beta$ -CD-AuNPs.

AuNPs exhibit applications as transfection vectors,<sup>187</sup> siRNA and DNA-binding agents,<sup>167,188</sup> protein inhibitors,<sup>189</sup> and spectroscopic markers.<sup>190,191</sup> A monolayer of thiolated CD derivatives, with different spacer lengths between the thiol termination and CD cavities, were adsorbed on gold films and described by many researchers.<sup>192,193</sup> The thickness and packing densities of the molecular monolayer as well as the orientation of the CD cavities and the outermost layers of these systems were controlled by changing the number of thiol groups and the length of the alkyl chain. The

**Table 7** Role of CD Complexation in Enhancing the Characteristics of the Loaded Bioactive Molecules

Year	CD Complex	Bioactive Molecule	CD Effect	Ref.
2005	Thiol derivatized $\beta$ -CD/AuNPs	Violacein (antitumor drug)	<ul style="list-style-type: none"> <li>Formation of (Violacein-<math>\beta</math>-CD-thiol-protected AuNPs) supramolecular system with higher cytotoxicity in vitro on V79 and HL60 cell lines.</li> </ul>	[183]
2009	SH-CD/AuNPs	$\beta$ -Lapachone (anticancer drug)	<ul style="list-style-type: none"> <li>Noncovalent encapsulation of the hydrophobic drug on CD-covered AuNPs (27 nm) carrier.</li> <li>Higher cellular uptake of drug-carrying CD/AuNPs was reported.</li> </ul>	[182]
2011	AuNPs@ Polyrotaxane	Doxorubicin	<ul style="list-style-type: none"> <li>Increases the loading capacity of the anticancer drug and enhances its controlled release.</li> </ul>	[176]
2013	Two-part arming system from per-6-thio- $\beta$ -CD coated AuNPs/adamantane oxoplatin conjugate	Cisplatin (Anticancer drug)	<ul style="list-style-type: none"> <li>4.7 <math>\pm</math> 1.1 nm delivery vehicle of Cisplatin from adamantane oxoplatin prodrug was obtained to produce cytotoxic nanodrug.</li> </ul>	[178]
2015	Ternary system of $\beta$ -CD- Phenylethylamine (PhEA) /AuNPs	Phenylethylamine (Antidepressant)	<ul style="list-style-type: none"> <li>The ternary system of <math>\beta</math>CD-PhEA-AuNPs, with AuNPs of 14 nm average size, enabled the effective photothermal drug release</li> </ul>	[181]
2020	$\beta$ -CD/chitosan/ Au nanocubes (AuNCs) hydrogel	Cytochrome c (mitochondrial protein)	<ul style="list-style-type: none"> <li>AuNCs were formed inside the 3-D inter-linked CS-g-<math>\beta</math>-CD hydrogel network for the protein immobilization.</li> <li>The mean edge length of AuNCs increased from 40.2 nm to 200–250 nm.</li> </ul>	[174]

substitution of all secondary hydroxyl groups in the  $\beta$ -CD rings by S-H groups afforded the synthesis of highly water-soluble AuNPs with the outermost layer formed by  $\beta$ -CD cavities. Using a spacer group between the S-H terminations in the preparation of NPs is novel. It could also increase the number of adsorbed  $\beta$ -CD molecules and improve particle size control. One of these modified AuNPs is capped with  $\beta$ -CD-alkyl thiol derivatives, mono [6-deoxy-6-[(mercapto-hexamethylene) thiol]]- $\beta$ -CD.

The inclusion complexation of certain hydrophobic drugs such as violacein, an antitumor drug, in  $\beta$ -CD-S(CH<sub>2</sub>)<sub>6</sub>-S-AuNPs afforded violacein transfer to an aqueous medium.<sup>183</sup> Cell viability measurements indicated that the system violacein-modified NPs maintained the violacein cytotoxicity on myeloid leukemia cells (HL60) and reduced the activity towards the normal cells (V79), ie, it became less cytotoxic on normal V79 cells compared to other violacein/ $\beta$ -CD complexes (Figure 6). Hence, this novel modified-NPs system enhanced the selectivity and targeting ability toward tumor cells.<sup>183</sup>

The conjugation of AuNPs by CD molecules occurs during the reduction process, using Na-borohydride in dimethylsulphoxide solvent. The obtained AuNPs-CD gold can be utilized as multisite hosts for binding other guests in the solution such as 1-adamantane and ferrocene methanol.<sup>173</sup>

Generally, a great interest has been directed toward developing and modifying nanomaterials as novel drug delivery systems.<sup>194</sup> The inorganic AuNPs were considered promising drug delivery and targeting carriers, especially for cancer treatment and phototherapy.<sup>119,195</sup> However, the application of such unmodified NPs for drug delivery is limited by the quick release of the loaded drugs from the surface of AuNPs, as well as their considerable cytotoxicity.<sup>196</sup> To overcome this limitation, the chemical modification of such NPs to relatively sustain the drug release is required. The modification of AuNPs with CD molecules is a famous example and had great interest from researchers in the last decade.<sup>197</sup> The modified complex system has the advantages of both CD (inclusion ability of different hydrophobic drugs, improving solubility and bioavailability and stability of the included drugs)<sup>198</sup> together with the advantages of AuNPs (increasing the drug selectivity and targeting to a specific site of action via the addition of targeting molecules)<sup>196,199</sup> making the combined new system as an attractive and promising approach for drug delivery.<sup>171</sup> Curcumin (CUR), a drug utilized for the prevention and treatment of osteoporosis, was loaded on AuNP-CDs by Heo et al.<sup>200</sup> It was noted that the modified NPs were spherical, ranging from 20 nm to 40 nm. Also, the obtained Au-CD loaded-CUR showed a better effect at lower concentrations compared with either the plain drug or the unmodified AuNPs.

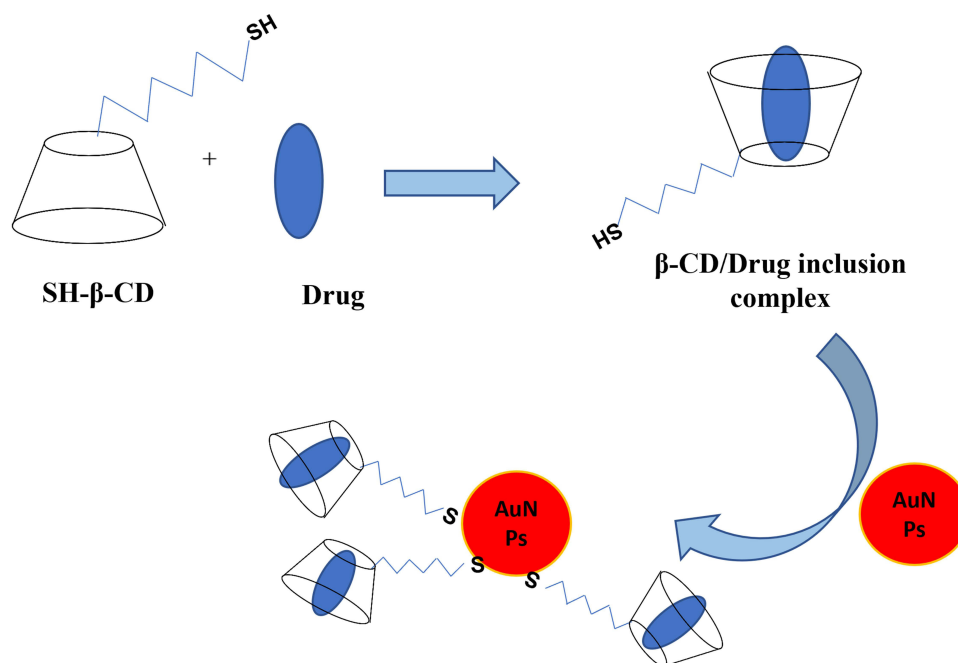


**Figure 6** Formation of the ternary system which is composed of the inclusion complexation of guest drug (eg, anticancer drug) in the  $\beta$ -CD cavity and then conjugation with gold nanoparticles ( $\beta$ -CD-S(CH<sub>2</sub>)<sub>6</sub>-S-AuNPs) for drug delivery.

Similarly, curcumin as an anticancer was loaded on the CD-NPs system via inclusion complexation and reported by Möller et al.<sup>201</sup> The results indicated that the modified system loaded with the drug exhibited a higher cytotoxic effect compared with the free drug. The complete inhibition of cancer cells was achieved within a few hours of incubation.

Baicalin (BC), as an anticancer cancer drug, has low cancer cellular uptake.<sup>200</sup> Therefore, AuNP@CDs were utilized as a drug carrier for (BC). The results illustrate that the modified AuNP-CD-BC solved the targeting problem since they inhibited cellular growth and induced apoptosis of all targeted cells upon using 100 mM drug concentration.<sup>202</sup>

Similar findings were obtained and reported previously on the high activity and selectivity of the modified paclitaxel (PTX)-loaded AuNP@CDs<sup>203</sup> and  $\beta$ -lapachone AuNP@CDs<sup>182</sup> for the treatment of cancer. Shi and his coworkers studied the impact of CD-coated AuNPs as a delivery carrier for a prodrug of cisplatin (Adamantane–Oxoplatin conjugate) to produce a cytotoxic nanodrug in vivo.<sup>178</sup> The inclusion complexation between CDs and adamantane moieties was utilized for the construction of a nanodrug with a stoichiometric ratio of 1:1. The results indicate CD decorating AuNPs play an important role in the increase of the photothermal potential of AuNPs as anti-tumor.

Silva and co-workers utilized the inclusion complexation of  $\beta$ -CD, coating AuNPs, for loading and controlled release of methotrexate (MTX) as an anticancer drug.<sup>204</sup> CDs enhanced the solubility and decreased the side effects of the drug. The drug was allowed to release from the modified system via laser irradiation of the cells, causing laser light absorption by AuNPs. Then, the absorbed light was transformed into heat dissipated into the environment. Consequently, this allowed the controlled release of the included drug from CD cavities. Afterward, the released MTX gives its cytotoxic effect. MTT assay was utilized for the investigation of HeLa tumor cell viability. The results showed that the irradiated cells with the modified ternary system caused huge cell growth inhibition. Table 8 lists the applications of CD-NPs for drug delivery and targeting.

**Table 8** Different Reported Drug Targeting/Delivery Applications of CD-AuNPs Complexes

Year	CD-AuNPs Complex	Drug	Biological Target	Results	Ref.
2005	Supramolecular system of $\beta$ -CD-Thiol-protected AuNPs ( $\beta$ -CD-S(CH <sub>2</sub> ) <sub>6</sub> -S-Au)	Violacein (antitumor drug)	<ul style="list-style-type: none"> <li>Normal (V79) fibroblasts cells derived from Chinese hamsters</li> <li>Human leukemia cells (HL60) cell lines</li> </ul>	<ul style="list-style-type: none"> <li>Formation of (Violacein-<math>\beta</math>-CD-thiol-protected AuNPs) supramolecular system with higher cytotoxicity in vitro.</li> </ul>	[183]
2014	AuNPs- $\beta$ -CD/ $\beta$ -D-galactose-recognizing lectins peanut agglutinin (PNA) and human galectin-3 (Gal-3)	Methotrexate	Lectins PNA and Gal-3	<ul style="list-style-type: none"> <li>CD enhanced the ability of AuNPs to load the anticancer drug providing a site-specific delivery system.</li> </ul>	[205]
2014	$\beta$ -CD/AuNPs	Curcumin	RANKL-induced BMMs	<ul style="list-style-type: none"> <li>The CUR-<math>\beta</math>-CD-GNPs complex:</li> <li>Elicited better effect at lower concentrations compared with the drug or the unmodified AuNPs alone.</li> <li>Improved bone density and prevented bone loss in vivo.</li> </ul>	[200]
2018	$\alpha$ -, $\beta$ -, and $\gamma$ -CD/ Polyethyleneglycol-Conjugated AuNPs	Curcumin	Human lung carcinoma cell line (A549 Cells)	<ul style="list-style-type: none"> <li>The three complexes elicited cytotoxic effects compared with the curcumin, which was not toxic.</li> </ul>	[206]
2016	AuNPs/thiolated $\beta$ -CD (AuNP-S- $\beta$ -CD)	Baicalin Anti-cancer drug	Cancer Foundation-7 (MCF-7) cells	<ul style="list-style-type: none"> <li>AuNP-S-<math>\beta</math>-CD-BC complex showed high proliferation inhibition effect on MCF-7 cells via inducing apoptosis.</li> </ul>	[202]
2015	CD dimmers, biotin-CD AuNPs-Ad moieties Targeting legend: (Biotin units)	Paclitaxel (Anti-cancer drug)	SKOV-3, NIH3T3, and NIH3T3 cell lines	<ul style="list-style-type: none"> <li>The complex showed active targeting of drug and improved its aqueous solubility, biocompatibility, and anticancer activity.</li> </ul>	[203]
2009	SH-CD/ AuNPs Anti-fouling shell: PEG Targeting moiety: Anti-EGFR	$\beta$ -Lapachone (Anticancer drug)	<ul style="list-style-type: none"> <li>MCF-7 (low glutathione concentration)</li> <li>A549 cells (high glutathione concentration).</li> </ul>	<ul style="list-style-type: none"> <li>The modified system containing CD provided suitable carriers of hydrophobic anti-cancer drugs.</li> <li>Anti-EGFR increased the cellular uptake of the modified nanosystem.</li> </ul>	[182]
2013	Two-part arming system from per-6-thio- $\beta$ -CD coated AuNPs/adamantane Oxoplatin conjugate	Oxoplatin prodrug releasing the Cisplatin anticancer drug	Human neuro- blastoma (SK-N-SH)	<ul style="list-style-type: none"> <li>Formulation of a delivery vehicle for the cytotoxic nanodrug Cisplatin from adamantane Oxoplatin prodrug.</li> </ul>	[178]
2018	AuNPs + $\beta$ -CD	Methotrexate	HeLa tumor cells	<ul style="list-style-type: none"> <li>Thermal irradiation produced photothermal controlled release of the drug from CD cavities, which increases its cytotoxicity.</li> </ul>	[204]

## $\beta$ -CD-Modified AuNP Aggregates

One of the properties of AuNPs is their ability to form nano-aggregates of specific surface plasmon resonance (SPR).<sup>207</sup> In fact, the random unintended aggregation of AuNPs is undesirable in general. However, the intended and planned aggregate formation was the subject of plenty of research articles in the last decade. In our review, we focused on some of these pharmaceutical and biomedical applications. AuNPs aggregates were formulated by different approaches including metal–ligand interaction,<sup>208</sup> ion–pair interaction,<sup>209</sup> hydrogen bonding,<sup>210</sup> and hydrophobic interaction via host–guest inclusion complexation<sup>166</sup> etc. There are several research articles discussing the formulation and applications of AuNP nano-aggregates, but only a few articles focus on aggregation reversibility and the factors that may affect such property, including pH change,<sup>211,212</sup> temperature change,<sup>213</sup> and biomolecular recognition.<sup>214</sup> For AuNPs aggregation, it is important to conjugate the nanoparticles with various materials, including proteins,<sup>215</sup> DNA,<sup>216,217</sup> synthetic polymers,<sup>213</sup> fullerenes,<sup>217</sup> and cyclodextrins (CDs)<sup>218</sup>.

Cyclodextrins are preferable over other materials because of their low toxicity, and high solubility. We study the complexation between  $\beta$ -CD, conjugating AuNPs, and diazo (guest).<sup>219</sup> Diazo molecules have a double azobenzene structure, acting as a crosslinking agent to bind the individual nanoparticles together (Figure 7). It was observed that the color of the gold colloid was changed upon aggregation into purple, accompanying the shift in the absorption spectrum. Also, the average number of AuNPs, in the constructed nanoaggregate depended on the amount of both CD and diazo. The dissociation of the formulated gold aggregates was realized via the addition of  $\alpha$ -CD, which acts as a competitive host to  $\beta$ -CD.

Hence,  $\alpha$ -CD formed new inclusion complexes with the utilized guest molecules by capturing them from the cavities of  $\beta$ -CDs. Interestingly, the recovery and self-assembling of AuNPs- $\beta$ -CD were achieved upon the addition of the guest molecules again. Therefore, the modified system is smart and reversible, which is controlled by the addition of either  $\beta$ -CDs or guest molecules.<sup>219</sup>

Also, the aggregate of AuNPs which were conjugated with thiolated CDs (SH-CD) was performed in an aqueous solution via the inclusion complexation between 1,10-phenanthroline (guest molecules, utilized as molecular retractor which binds the nanoparticles together) and BCD (host molecules). The modified system was characterized by different analysis techniques including fluorescence, FT-IR, and UV spectroscopy. The results showed that the aggregation process depends on the concentration of both guest and CD molecules.<sup>220</sup>

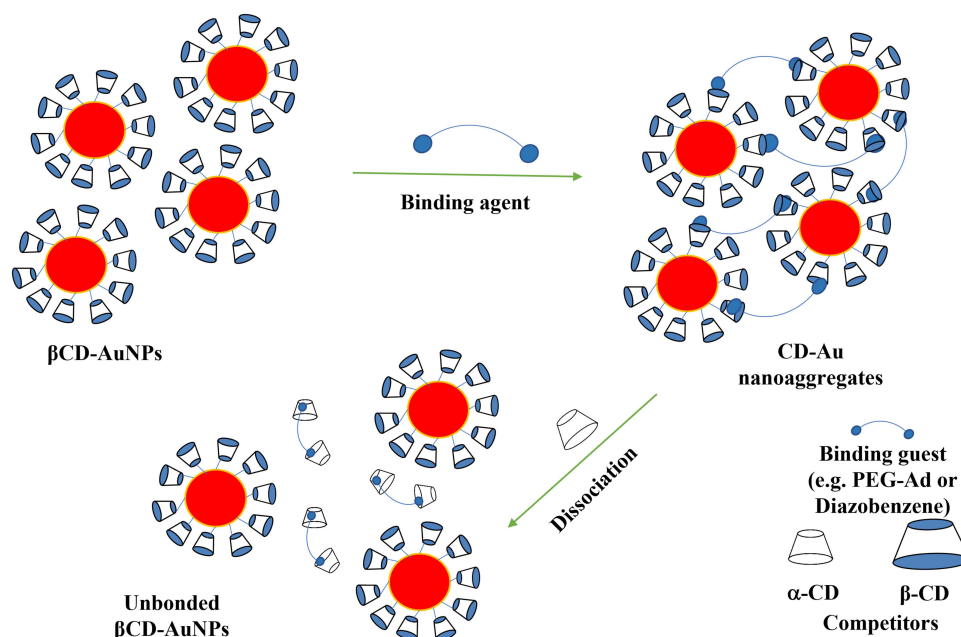


**Figure 7** The representation of the aggregation and the competitive dissociation of smart AuNPs- $\beta$ -CD via the addition of either guest molecules (ie, PEG-Ad or diazo) causing aggregation, or  $\alpha$ -CD as competitor host molecules.

## Role of Cyclodextrin in Gene-Drug Delivery (DNA Concentration)

Cyclodextrins are helpful in gene delivery applications because of their binding affinity to nucleic acids and their ability to reduce the cytotoxicity of other gene carriers.<sup>221,222</sup> CD-containing polymers were demonstrated by Davis for DNA aggregation. The modified system is a highly biocompatible matrix for recombinant adenovirus-mediated gene delivery to local wound sites.<sup>223</sup> Another research article showed the utilization of CDs in the improvement of adenoviral-mediated gene transfer into the jejunum of rats.<sup>224</sup> CDs can bind various molecules via the formation of inclusion complexes.<sup>225</sup> Therefore, CDs have been used to construct supramolecular aggregates acting as receptors in biological technology. In addition, cyclodextrins are considered effective absorption and gene-delivery enhancers. An earlier study showed the utilization of CDs in improving adenoviral-mediated gene transfer into the jejunum of rats.<sup>224</sup> The obtained improvement was attributed to CD molecules in the gold NPs, which enhanced the viral binding and subsequent internalization into the host cells. Moreover, the derivatization of CD at the 6-position was reported for the improvement of plasmid DNA (32P-labeled pDNA) complexation capacity and consequent cellular uptake efficiency as in the case of COS-7 cell transfection.<sup>226</sup>

It was reported that adamantane (Ad) forms perfect inclusion complexes with  $\beta$ -CD. This kind of complexation has been utilized in the construction of self-assembling nanoparticles.<sup>227</sup> As a nonviral vector, the CD-based polycations have been synthesized to deliver DNA.<sup>223,228</sup> These polycationic polymers can be self-assembled with DNA molecules via electrostatic interactions to form nano-assembly which are called “polyplexes.” The modified NPs exhibited higher cellular internalization of the gene compared with unmodified DNA.<sup>229,230</sup> The modified polyplexes, based on CD, were specifically immobilized on Ad-functionalized surfaces via inclusion complexation. Compared to PEI-modified NPs, CD-PEI NPs showed noticeably greater adsorption on Ad surfaces. Additionally, compared to single CD molecules, the combined CD-PEI NPs have a greater binding affinity Ad surface due to multivalent interactions. On the other hand, the immobilized NPs, illustrated in [Figure 8](#), were examined by AFM and fluorometric spectroscopy.<sup>231</sup>

Oligo (ethylenediamine)- $\beta$ -CD-modified AuNP (OED-CD-NP) was constructed as a non-viral vector for DNA.<sup>232</sup> The aggregation behaviors of these constructed systems with DNA were characterized by several microscopic and spectroscopic techniques. The obtained results indicated a direct relationship between the morphological feature of the modified aggregate and the initial concentration of both OEA-CD-NPs and DNA. The transfection efficiency of the modified system was evaluated by MTT assay using MCF-7 cells. The obtained results indicated the successful delivery of noroviral vectors into the cancer cells. In contrast, the system free of CD molecules had a weak bond with the DNA receptor, indicating the importance of CD in the modified system.<sup>232</sup>

Several AuNPs-capped CDs have been reported by different groups for application in gene delivery.<sup>17,233,234</sup> These studies focus on the construction and characterization of CD-AuNPs. The utilization of cyclodextrin-containing cross-linked matrixes for DNA aggregation has been established and reported by Davis and coworkers.<sup>223</sup> The modified cyclodextrin-based system was regarded as a highly biocompatible matrix for gene delivery. [Table 9](#) displays the effect of CD on gene delivery using AuNPs.

## Role of CDs in Preparation and Improvement of Catalytic Enzymes

Cyclodextrin-gold NPs were utilized to enhance the loading efficiency, control the release, and targeting of enzymes. Accordingly, different studies presented that CD-AuNPs are considered attractive and promising building blocks for effective artificial enzyme model engineering.<sup>236</sup>

For example, an artificial enzyme model was developed via the complexation of metal catalytic centers with  $\beta$ -CD modified AuNPs. Firstly, AuNPs were coated with SH-CD molecules. Secondly, the constructed CD-AuNPs were utilized as a backbone to install metal catalytic centers via self-assembling or inclusion complexation between adamantane-modified copper-triethylenetetramine complex and  $\beta$ -CD cavities, which act as hosts for adamantane guest molecules.<sup>236</sup> The results showed that in the prepared system, enzyme has catalytic behaviors, which were considered as an esterase mimic enzyme. Besides, the prepared enzyme exhibited excellent hydrolysis ability for catalyzing the breakdown of an active ester 4,4'-dinitro-diphenyl carbonate.

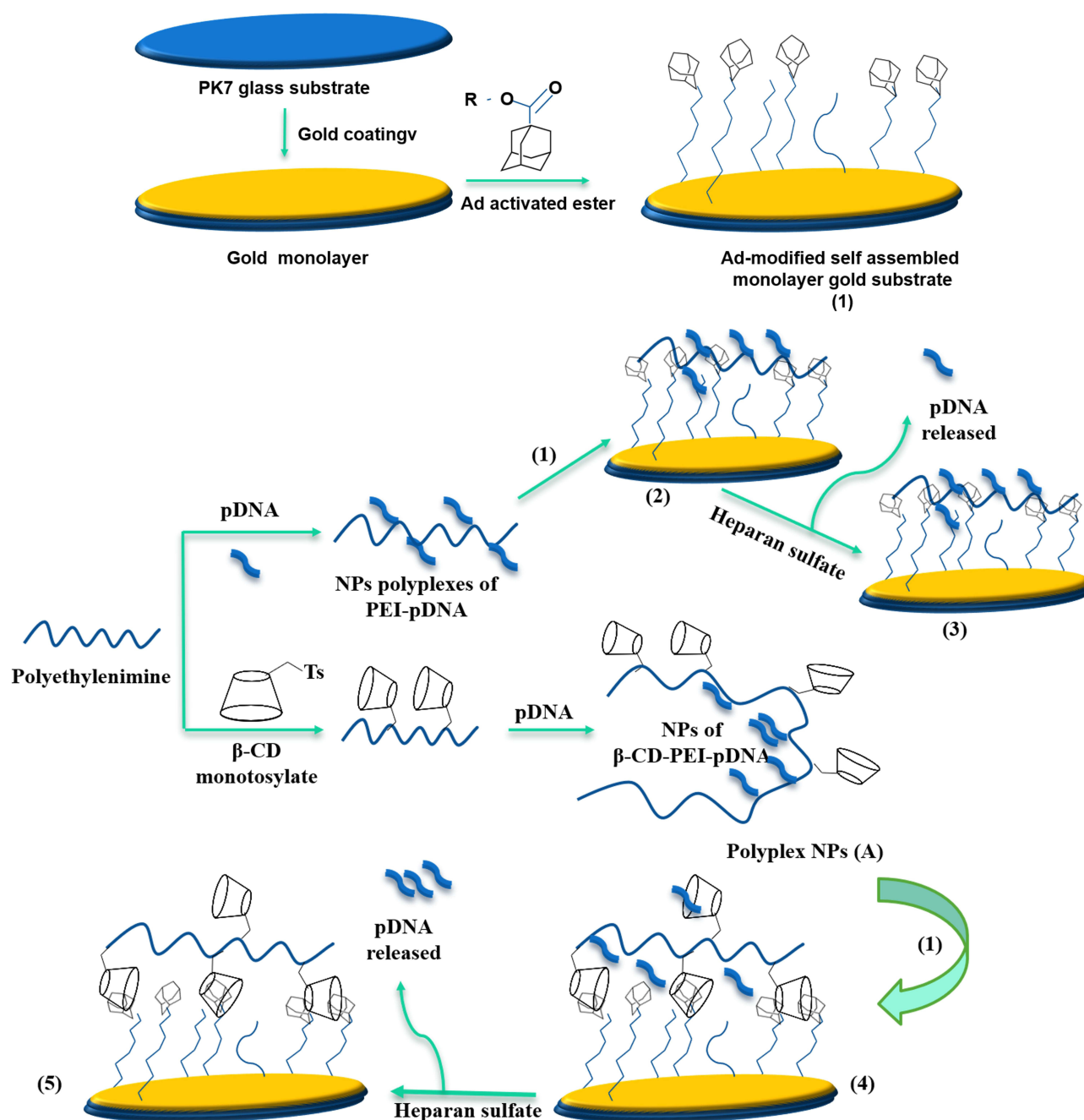


**Figure 8** Schematic representation of CD-AuNPs immobilization on Ad substrate via inclusion complexation for pDNA concentration according to the following steps. (1) Ad-modified self-assembled monolayer (SAM) gold substrate; (2) Immobilization of PEI-pDNA polyplex NPs on the modified SAM; (3) pDNA using Heparane; (4) Immobilization of  $\beta$ -CD-PEI-pDNA polyplex NPs on the modified SAM; (5) pDNA using Heparane.

Similarly, the host-guest supramolecular interactions were utilized by other researchers to formulate enzyme nanocatalysts.<sup>237,238</sup> The immobilization of enzymes (proteins) on the CD-containing AuNPs system was achieved via the inclusion complexation of one or more of the protein bulky moieties and the hydrophobic cavities of CD. Alternatively, the loading of the enzyme can be done by linking a hydrophobic moiety, such as adamantane molecules to the enzyme. Hence, the loading can be carried out via the inclusion of complexation between Ad molecules and CDs.

Additionally, the Ad/CD inclusion complexation was utilized for the formulation of nanodevices acting as biosensors. The modified system was conjugated with superoxide dismutase and catalase enzymes. The conjugation or loading of these enzymes was carried out by decorating these enzymes with adamantane moieties, which will be included in the CD

**Table 9** Effect of CD on Gene Delivery Using AuNPs

Year	CD Mediated Vector for Gene Binding	Gene	CD Effect	Ref.
2007	Oligo(ethylenediamino)- $\beta$ -CD-modified AuNPs (OEA-CD-NPs)	DNA	• CD deep cavities on the surface of OEA-CD-NPs aggregate prevented the deposition of Au clusters on cell membranes, which helped in decreasing their cytotoxicity.	[232]
2009	$\beta$ -CD/Pluronic Cationic Polyrotaxanes	DNA	• Novel cationic polyrotaxanes increasing the loading capacity, cytotoxicity, and gene transfection efficiency of DNA to cancer cells.	[179]
2014	$\beta$ -CD-AuNPs/ capped with anthryl adamantanes	Calf thymus DNA	• Form supramolecular nanostructure for the condensation of the DNA producing condensates of a suitable size for endocytosis by hepatoma cells.	[235]
2016	G5 dendrimer of poly(amidoamine)/ $\beta$ -CD-entrapped Au NPs (Au DENPs- $\beta$ -CD system)	Plasmid DNA (pDNA)	• $\beta$ -CD increases the cytotoxic effect of the Au DENPs- $\beta$ -CD system and enables more efficient cellular gene delivery than the system free of $\beta$ -CD.	[233]
2018	$\beta$ -CD-modified dendrimer-entrapped AuNPs (Au DENPs- $\beta$ -CD system)	siRNA	• The modified Au DENPs- $\beta$ -CD system enhanced the uptake (cytocompatibility) of siRNA into glioblastoma cells as well as its gene silencing, forming an effective gene therapy system for the inhibition of the expression of Bcl-2 and VEGF proteins.	[234]

cavities. The results of the analysis indicated the successful construction and development of the biosensor, based on Ad-modified bi-enzymatic nanodevice.<sup>237,239</sup> The same method was utilized for the formulation of uni- and bi-enzymatic nanocatalysts reported by another research group.<sup>81,238</sup> Ad-COOH was utilized for making hydrophobic capping of catalase enzymes to be immobilized on  $\beta$ -CD-AuNPs via supramolecular associations, and then the enzymatic nanocatalyst was further constructed via co-immobilization of  $\beta$ -CD-modified-dismutase (copper/zinc superoxide dismutase enzyme).<sup>81</sup> The results showed that the modified system still retained about 35% and 73% of initial specific activity for dismutase and catalase, respectively. It was also observed that the thermal stability was improved by the process of co-immobilization. Additionally, the bi-enzymatic immobilization with catalase on metal nanoparticles improved the resistance efficacy of superoxide dismutase by 90-fold to the inactivation by  $H_2O_2$  (at a concentration of 100 mM).<sup>81</sup>

Recently, thiolated  $\beta$ -CD-AuNPs supramolecular associations (water soluble) have been utilized to immobilize native or Ad-modified enzyme structures through host-guest interactions. For example, the enzyme L-phenylalanine dehydrogenase (PhDH) modified by Ad-carboxylic acid (Ad-PhDH) was immobilized on  $\beta$ -CD-AuNPs via supramolecular interactions. The results revealed that the formulated enzyme retained its catalytic activity and affinity to the substrate.<sup>239</sup> Noteworthy, AuNPs, and CD derivatives have catalytic capacity, which mainly comes from guest molecules.<sup>171</sup> Table 10 lists the selected studies on some CD-AuNPs complexes used for the preparation and improvement of catalytic enzymes.

**Table 10** Selected Studies on Some CD-AuNPs Complexes Used for the Preparation and Improvement of Catalytic Enzymes

Year	CD-AuNPs Complex	Enzyme	Role	Ref.
2005	$\beta$ -CD-AuNPs Supramolecular assembly	Bovine pancreatic trypsin	• Successful supramolecular immobilization of trypsin.	[238]
2005	$\beta$ -CD-AuNPs	Catalase and Copper/Zinc superoxide dismutase enzymes	• Successful supramolecular co-immobilization of both enzymes, improving their activity and thermal stability.	[81]
2006	$\beta$ -CD-AuNPs	Native and adamantane-modified L-Phenylalanine dehydrogenase	• Successful supramolecular immobilization of the investigated enzyme retaining its catalytic activity and the affinity to the substrate.	[239]
2008	TEA-Ad- $\beta$ -CD- modified AuNPs with metal ( $Cu^{2+}$ ) catalytic centers (Artificial nanozyme model)	Artificial catalytic nanozyme for the hydrolysis of the activated ester DNDPC.	• The nanozyme system showed strong hydrolysis activities for the active ester DNDPC.	[236]
2016	$\beta$ -CD-AuNPs (15–20 nm)	Glucose oxidase (GOx)	• $\beta$ -CD-AuNPs complex formed nano-platform for sensing, self-assembly, and cascade catalysis with mimicking properties of both glucose oxidase and horseradish peroxidase simultaneously.	[240]
2017	$\beta$ -CD-AuNPs	PNi@IPTS-Azo@ $\beta$ -CD-AuNPs catalytic substrate	• High efficiency, regenerative, material-saving, catalytic model was obtained from the inclusion complexation between CD and Azo benzene moieties. • The modified system was considered as catalytic fixed beds suitable for industrial applications.	[241]
2020	$\beta$ -CD-AuNPs (Co-catalyst)	$Cu^{2+}$ -PPI + $H_2O_2$ inorganic pyrophosphatase (PPase)	• The modified system acted as co-catalyst Improves the colorimetric and photothermal biometric properties via improving the $Cu^{2+}/Cu^+$ conversion rate.	[242]

**Abbreviations:** TEA-Ad, triethylnetetramine-Adamantane; DNDPC, 4,40-dinitrodi-phenyl carbonate; PNi, Porous nickel; IPTS, (3-isocyanatopropyl) triethoxysilane; Azo, azobenzene; PPI, inorganic pyrophosphate.

## Role CD-AuNPs in the Formation of Self-Assembling Molecular Print Boards

Owing to their high binding strength and reversibility,<sup>111,243</sup> the inclusion complexation has been utilized for the construction of receptor-functionalized molecules and nanoparticles called molecular print boards. The concept of “molecular print boards” was introduced by the Reinhoudt group,<sup>244</sup> which are  $\beta$ -CD self-assembled mono- and multi-layers on silicon oxide or gold substrates that possess supramolecular host properties.<sup>245,246</sup>

The inclusion complexation between adamantane (Ad) and cyclodextrin cavities was utilized for the construction of physical nano assemblies. Huskens and his co-workers reported that Ad-end capping polypropylene imine dendrimer Ad-PPI, ranging from 4 to 64 Ad moieties, act as guest molecules, which will be included in the cavities of CD-decorating AuNPs (host molecules)<sup>247</sup> to form self-assembled monolayer molecular print board, as illustrated in (Figure 9). Upon using multiple inclusion complexes between CD and Ad (Ad-CD) stable assemblies can be obtained of high strength. The modified structural surfaces can be utilized for different nanotechnological and electronic applications. Also, the modified systems can be utilized as molecular print boards on which the molecules can be firmly placed.<sup>247</sup>

Similarly, a novel multi-layered, self-assembled organic-metal NP was constructed via layer-by-layer assembly. The modified nano-assembly was characterized by UV and SPR spectroscopy as well as atomic force microscopy. The results indicated a direct relationship between the number of bilayers and the extent of absorption. Various structures of multiple supramolecular interaction assemblies might be obtained via such protocols. This provides a general pattern for nanofabrication via integrating several components from inorganic, organic, metallic, and bio-molecular reagents while maintaining the specificity of supramolecular interfacing.<sup>248</sup> Previously, this group of researchers also studied the irreversible precipitation of dendrimer/CD-AuNPs aggregates induced by the complexation of a CD-modified AuNPs solution with adamantyl dendrimers.<sup>249</sup>

Other research groups<sup>250,251</sup> demonstrated nanostructures of supramolecular layer-by-layer assembly of 3D multi-component nanoparticles. Generally, there are two classes of nanofabrication methods: “top-down” and “bottom-up.”

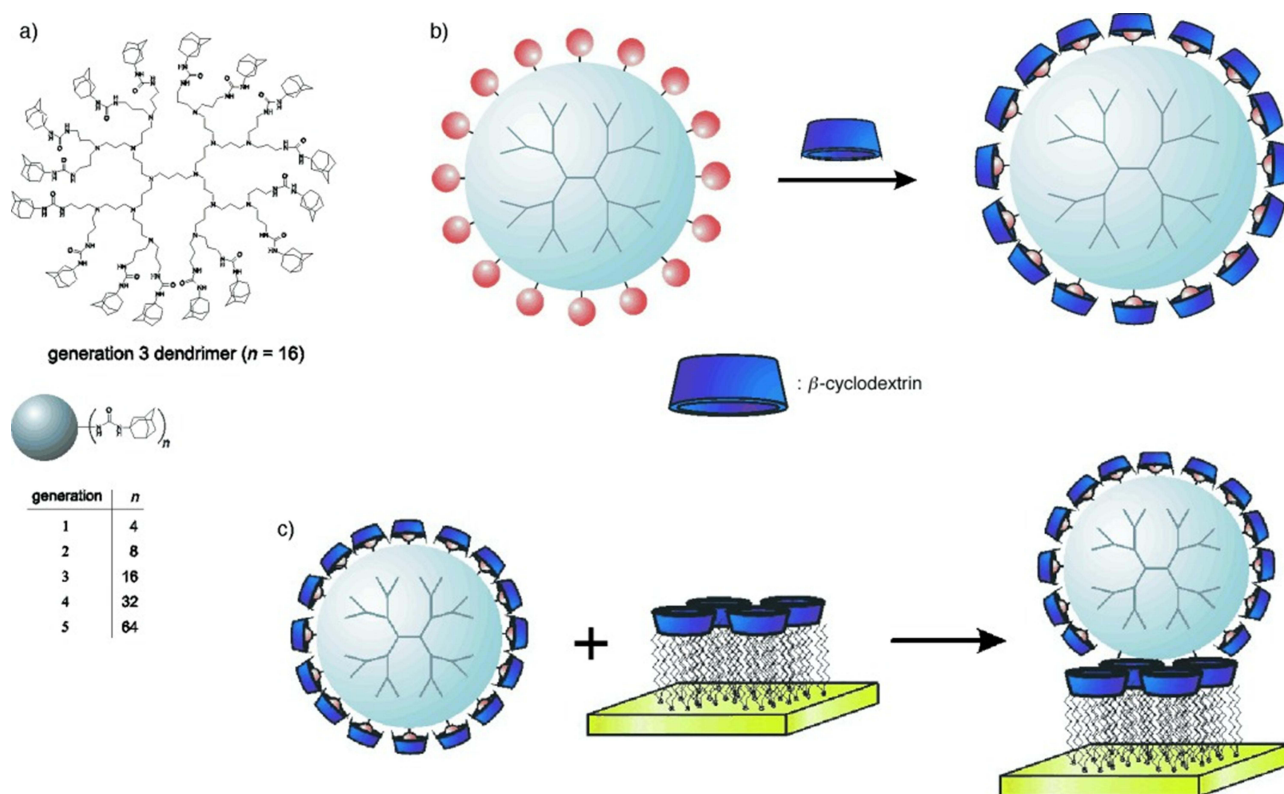


**Figure 9** Chemical structures of adamantly functionalized PPI dendrimers (Ad-PPI) and their formation of inclusion complexes with cyclodextrins to construct water-soluble assemblies (A); the formation of a monolayer of these modified assemblies on a gold substrate via adsorption (CD-AuNPs monolayer) (B); and formation of multilayer CD-assemblies on gold (C). Reproduced with permission from Copyright 2002 Wiley VCH GmbH.<sup>247</sup>

There are different\common techniques utilized in the case of the “top-down” class method, including directed self-assembly, supramolecular assembly, and probe lithography techniques. On the other hand, soft lithography, lithography, and evaporation techniques are common examples of the ‘bottom-up’ class (Figure 4). Layer-by-layer assembly and nanoimprint lithography (NIL) were used as tools of patterning that fabricated patterned  $\beta$ -CD-SAMs complexes and retained nanoparticles on the substrate. In addition, a combination of metallic and inorganic NPs with organic molecules built-up multi-layered and multicomponent NP arrays ie, CD-conjugated gold NPs (CD-Au,  $d \sim 3$  nm), CD-coated silica NPs (CD-SiO<sub>2</sub>,  $d \sim 350$  nm), ferrocenyl-coated silica NPs (Fc-SiO<sub>2</sub>,  $d \sim 60$  nm), and adamantyl-end-capping poly (propylene imine) dendrimers (G1-PPI-(Ad)<sub>4</sub> (generation 1). The gathering of guest- and host-functionalized NPs appeared in a layer-by-layer alternating assembly (Figure 10).

Furthermore, the ordering effects of the steps of nanoparticle assembly including, small-to-large and large-to-small nanoparticle assembling were compared. Interestingly, supramolecular LbL assembly provided control nanostructures over their height in the nanometre range, whereas NIL provided confinement nanostructure in the x and y directions. Full integration of these methods, therefore, lead to the fabrication of arbitrary shape from 3D nanostructures on substrates.<sup>251</sup>

Also, multiple inclusion of the guests (adamantane end capping polyisobutene-alt-maleic acid polymer) into the cavities of  $\beta$ -CD self-assembled monolayers were constructed and reported by Crespo-Biel and co-workers.<sup>252</sup> The results indicated that the adsorption was irreversible, strong, and specific. Also, the polymer adsorption led to very thin polymer films on the surface as evidenced by both SPR spectroscopy and AFM. Moreover, the results indicated that there is no significant effect of the selected hydrophobic moieties (nature and number) decorating the polymer as well as the polymer concentration on the adsorption capacity.

## Role of CD-AuNPs in the Fabrication of Supramolecular Functionalized Electrodes and Biosensors

Another novel application of  $\beta$ -CD-capped gold NPs is the development of a supramolecular-functionalized redox electrode acting by the physical assembly between  $\beta$ -CD coating AuNPs ( $\beta$ -CD-AuNPs) and ferrocene moieties coating indium tin oxide (Fc-ITO)<sup>253</sup> Cyclic voltammetry and AFM evaluated the immobilization of  $\beta$ -CD-AuNPs on the Fc-ITO vehicle. In addition, cyclic voltammetry confirmed the supramolecular characteristics of the immobilization process. CD-modified

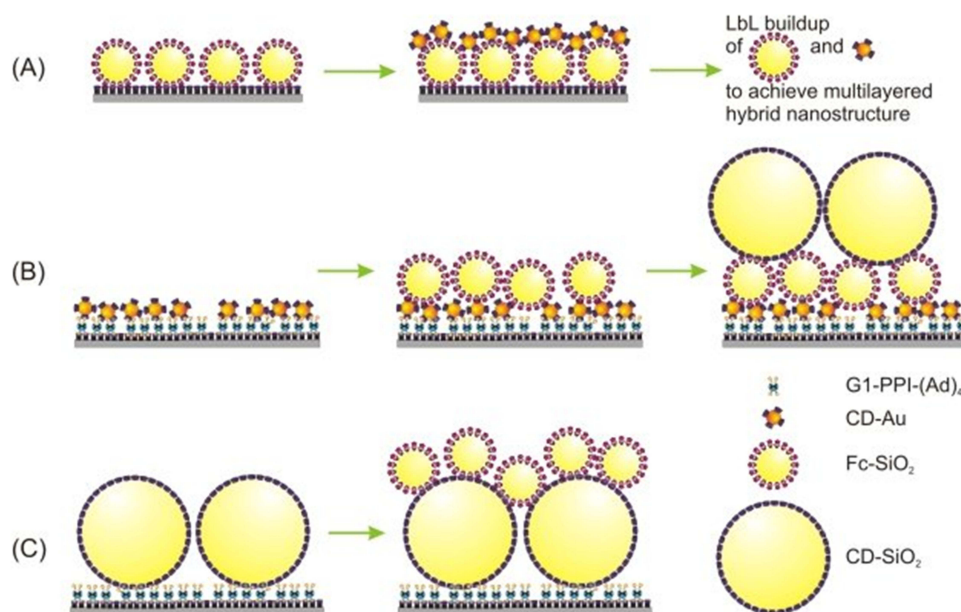


**Figure 10** Schematic representation of the multicomponent nanostructures construction using (A) CD-Au and Fc-SiO<sub>2</sub>; (B) The nano-assembly from small NPs to large NPs; and (C) nano-assembly from large NPs to small NPs. The artwork was reproduced from MDPI according to permission via license: CC BY 4.0.<sup>251</sup>

electrodes exhibited enhanced electrocatalytic and electroanalytic effects compared to the unmodified (CD-free) Fc-ITO-electrode toward the ascorbic acid.<sup>253</sup>

CDs possess a special structure that enables them to generate polymers of various structures that perform different functions via several reactions,<sup>199</sup> as well as in synergy with inorganic nanoparticles.<sup>254</sup> Furthermore, entrapping of drugs via complexation with CDs improves their stability and bioavailability.<sup>198</sup>

Interestingly, immersing the modified electrode in a saturated solution of adamantane carboxylic acid (Ad-COOH) leads to the disruption of the modified system. This may be because the adamantane moieties have a higher affinity to CD cavities and can form highly stable complexes with  $\beta$ -CD compared to Fc, causing the release of  $\beta$ -CD-AuNPs from the electrode surface. The obtained findings confirm that the immobilization mechanism depends on the previously described inclusion complexation hypothesis.<sup>253</sup>

Bisphenol A (BPA) is an organic material used to manufacture polycarbonate plastics and epoxy resins, which are subsequently utilized for coating the internal surfaces of cans. Bisphenol A can disrupt the human health endocrine system. Therefore, it is important to detect its amount in the environment. A new molecular imprinted system was constructed from acryloyl- $\beta$ -CD, acrylamide (AAM), and N, N-methylene bis-acrylamide (MBAA). Then, it was loaded with bisphenol, as illustrated in. The modified system was utilized as a sensor for the detection of bisphenol.<sup>155</sup> In this concern, bisphenol can be detected potentiometrically by monitoring the change in the color of the hydrogel system from blue to red. The modified system can detect bisphenol at a concentration of 0.5 mM.<sup>155</sup>

An ultrasensitive detection of bisphenol A was also described and previously published.<sup>255</sup> The detection was carried out by utilizing an electrochemical biosensor, constructed from graphene oxide-AuNPs decorated with  $\beta$ -CD molecules. Then, the system was heated and electrodeposited to obtain a glassy carbon electrode. The modified biosensor was characterized by different analyses, including X-ray (XRD), UV, and SEM. The results exhibited a good detection limit of bisphenol ( $3 \times 10^{-9}$  M) with high stability.<sup>255</sup>

Similarly, an electrochemical biosensor was reported by Wu et al,<sup>256</sup> the modified system was constructed from the deposition of  $\beta$ -CD-AuNPs on stainless steel electrodes. The constructed system was utilized for the detection of low-density lipoprotein (LDL). In the modified system,  $\beta$ -CD was utilized as a binding receptor for LDL via different binding mechanisms including van der Waals forces, hydrophobic interactions, and hydrogen bonding. The results indicated that the modified  $\beta$ -CD-AuNPs biosensor exhibited a high sensitivity towards LDL.

Moreover, thiolated  $\beta$ -CD-AuNPs with reduced graphene oxide were modified and utilized for both acetaminophen and ofloxacin electrochemical sensing. The results showed that the detection limits for acetaminophen and ofloxacin were  $3 \times 10^{-8}$  M and  $8 \times 10^{-9}$  M, respectively. In addition to its wide detection range, the sensor showed high stability, and reproducibility.<sup>198</sup>

Hydrogen peroxide ( $H_2O_2$ ) biosensors were synthesized by incorporating AuNPs into the cyclodextrin/chitosan hydrogels. Noteworthy,  $H_2O_2$  shares in mitochondrial electron transfer reactions. Also, this kind of oxygen species is considered the most stable one which can penetrate the cell membrane and damage the cell proteins. Hence, the detection of  $H_2O_2$  level changes is very important. The results showed that the presence of AuNPs in such modified hydrogels improved the conductivity. Consequently, we improve the biosensor sensitivity with a low detection limit for  $H_2O_2$  and its cell biocompatibility.<sup>201</sup>

Moreover, a chemo-visual biosensor based on AuNPs-polymerized CD was constructed and reported by Lee et al for the detection of both cysteine and sodium diethyldithiocarbamate (SDDC).<sup>202</sup> The CD polymer acts as a stabilizer and reducing agent to form small AuNPs of about 15 nm. The results illustrated that the color of AuNPs was changed from red to blue upon attaching sodium diethyldithiocarbamate (SDDC) and cysteine as sulfated compounds. It was realized that the role of CD, as an amphiphilic structure, was the agglomeration of AuNPs and the entrapment of the sulfated compounds. The modified sensor detection limits were 0.05 and 0.07  $\mu$ M for SDDC and cysteine, respectively. Table 11 lists some selected studies on the fabrication and applications of supramolecular functionalized electrodes based on CD-AuNPs complexation.

**Table II** Selected Studies on the Fabrication of Supramolecular Functionalized Electrodes Using CD-AuNPs Complexation

Year	Functionalized / Modified Biosensor	System Composition	Detected probe	Role of CD-AuNPs Conjugation	Ref.
2008	Supramolecular recognition functionalized redox electrode	$\beta$ -CD- AuNPs Ligand electrode: Fc-ITO	Ascorbic Acid	<ul style="list-style-type: none"> <li><math>\beta</math>-CD- AuNPs complexation improved the electrocatalysis activity of Fc-ITO electrode towards ascorbic.</li> </ul>	[253]
2009	Amperometric glucose sensor (AuNPs/CD-Fc/GOD)	Mono-6-thio- $\beta$ - CD- AuNPs Ligand: Ferrocene (Fc) capped on AuNPs and GOD	Glucose	<ul style="list-style-type: none"> <li>CD/AuNPs complexation formed an electron shuttle and allowed the detection of glucose at 0.25 V, which provided high stability, anti-interference ability, and natural life of the biosensor.</li> <li>AuNPs/CD-Fc film provides a convenient electron tunneling between the protein and the electrode, which provides excellent sensitivity.</li> </ul>	[257]
2012	$\beta$ -CD stabilized AuNPs detector	$\beta$ -CD-AuNPs	Micromolar quantities of $Pb^{2+}$ ions	<ul style="list-style-type: none"> <li>The deprotonated secondary OH group of <math>\beta</math>-CD provided the highest chelating affinity toward <math>Pb^{2+}</math> ions, which induces AuNPs aggregation.</li> <li>Aggregates changed the visual color from red to blue.</li> </ul>	[152]
2013	Enzyme electrode constructing reagentless amperometric 3D-biosensor	Au-Pt NPs- $\beta$ -CD-branched cysteamine core PAMAM G-4 dendron	Adamantane-modified GOD	<ul style="list-style-type: none"> <li>The supramolecular associations of AuNPs with inorganic-organic hybrid constructed a stable and highly sensitive biosensor with a low detection limit, and a rapid amperometric electroanalytical response to Adamantane-modified GOD.</li> </ul>	[258]
2016	GCE (Electrochemical sensor)	$\beta$ -CD-AuNPs Ligand: RGO	Electrocatalytic oxidation of BPA	<ul style="list-style-type: none"> <li>The modified sensor showed a perfect linear relationship between the detection current and BPA concentration.</li> </ul>	[255]
2018	Enzyme-free $\mu$ PAD biosensor loading secondary antibodies or peptide.	$\beta$ -CD Au-PWE	Two tumor markers; CEA and PSA antigens	<ul style="list-style-type: none"> <li>The Au-Paper based electrode showed high sensitivity, wide linear ranges, and low detection limits.</li> </ul>	[259]
2019	Plasmonic biosensor	$\beta$ -CD-AuNPs	Cholesterol	<ul style="list-style-type: none"> <li>Ultra-sensitive and highly integrated plasmonic biosensor with a promising localized surface, plasmon resonance properties, and ultralow detection limit of cholesterol.</li> </ul>	[260]
2019	Electrochemical sensor	Thio-b- $\beta$ -CD-functionalized graphene/AuNPs	Tetrabromobisphenol A in water	<ul style="list-style-type: none"> <li>Sensitive, reproducible, and selective sensor, showing linear range of low detection limits.</li> </ul>	[261]
2020	Colorimetric nanoprobe	$\beta$ -CD-AuNPs	Cysteine	<ul style="list-style-type: none"> <li>Obvious color change from wine red to purple was achieved by the decrease in the surface plasmon resonance band.</li> </ul>	[262]
2021	Electrochemical Biosensor	$\beta$ -CD-AuNPs	Low-density Lipoprotein	<ul style="list-style-type: none"> <li>A highly selective and sensitive biosensor with excellent molecular recognition performance, especially in ultra-low concentrations.</li> </ul>	[256]
2021	Multi-sensing colorimetric probe	$\beta$ -CD-AuNPs	Hydroxychloroquine drug	<ul style="list-style-type: none"> <li>Complexation of the drug with the probe causes red shifting in the surface plasmon resonance owing to the AuNPs aggregation.</li> </ul>	[153]
2021	Electrochemical catechol biosensor (Tyrosinase-based nanosensor)	$\beta$ -CD-AuNPs on graphite electrode Drug inhibition platform: Tyrosinase with the catechol substrate	Catechol	<ul style="list-style-type: none"> <li>The biosensor showed excellent capability for Tyrosinase inhibition by ibuprofen.</li> </ul>	[263]
2022	RVFT test box device	$\beta$ -CD-AuNPs (silver stained) NC-LPS. <b>Labeled protein:</b> SPA. <b>Test:</b> Brucella LPS. <b>Control:</b> Sheep IgG.	<i>Brucella</i> LPS	<ul style="list-style-type: none"> <li>The complexation provides an RVFT device that provides a short reaction time (5–6 min visible to the naked eye), without any equipment for the convenient, fast, effective, and inexpensive diagnosis of Brucellosis.</li> </ul>	[264]

**Abbreviations:** Fc-ITO, ITO coated with ferrocene residues; GOD, Glucose oxidase; RGO, Reduced graphene oxide; GCE, Glassy carbon electrode; BPA, Bisphenol A;  $\mu$ PAD, Microfluidic paper-based analytical device; Au-PWA, AuNPs modified paper working electrode; CEA, carcinoembryonic antigen; PSA, prostate-specific antigen; RVFT, Rapid vertical flow technology; NC, Nitrocellulose film; LPS, purified lipopolysaccharides; SPA, *Staphylococcus* protein A; IgG, Immunoglobulin.

## Cyclodextrin as a Phase Transfer Agent

Ferrocene is an excellent guest molecule to be included in CD cavities via hydrophobic–hydrophobic interaction. The inclusion of complexation between ferrocene derivatives and CD molecules conjugating AuNPs has received much attention in recent years. The binding interactions of AuNPs were utilized to transfer the hydrophilic CD-modified NPs (hydrophilic) into less polar solution phases. Therefore, CD molecules play an important role in the phase transition, which acts as a phase transfer agent. From these ferrocene derivatives, both dodecyl ferrocene and hexadecyl ferrocene act as phase transfer agents, facilitating the solubility of AuNPs in an organic solvent, such as chloroform.<sup>118</sup> However, other ferrocene derivatives have a limited ability to act as phase transfer agents such as heptyl-ferrocene and propyl-ferrocene derivatives. This may be due to

these derivatives having very limited amphiphilic properties. Therefore, the existence of CD molecules in the nano assemblies of gold could include the amphiphilic ferrocene moieties, which lead to phase transition via solubilization of the aqueous NP in chloroform.<sup>118,120</sup> Also, it was proved that AuNP@CDs had the ability to reversible-phase transfer between the aqueous phase and the organic phase by UV and Vis light irradiation.<sup>171,265</sup>

## Inclusion of Fullerenes

Fullerenes, special water-insoluble  $\pi$ -electronic systems, comprise lots of unsaturated carbon atoms linked to each other by single or double bonds to form hollow tubes or ball-like sphere structures. Fullerenes, also called Buckminsterfullerenes” show various interesting magnetic, superconductive, electrical, and biochemical properties.<sup>266,267</sup>

Because fullerenes C60 (cage-like structure composed of 60 carbon atoms) is extremely water-insoluble, the water-soluble gold NPs conjugated with thiolated  $\gamma$ -CD hosts were utilized to solubilize such kind of fullerene via inclusion complexation between fullerenes and the cavities of CDs to form a large soluble nanoaggregates as illustrated in Figure 11.

Additionally, because the method of fullerenes preparation is based on the thermal reactions of the appropriate carbon sources under various conditions,<sup>268</sup> the produced fullerenes are always obtained as a mixture of C60, C70, and higher homologs. Consequently, the separation of fullerenes from each other will be considered a challenge and a point of research for chemists. Water-soluble gold NPs modified with thio [2-(benzylamine) ethyl-amino]- $\beta$ -CD are constructed and successfully used as a selective recycling extractor for the C60 fullerene analog. The mechanism of separation is based on the fact that  $\beta$ -CD can only form an inclusion complex with C60 (at a ratio of 2:1 CD:fullerene) but cannot form such inclusion complexes with either C70 or the higher fullerene molecules.<sup>269</sup> Thus, C60 can be easily separated from the mixture of C60 and others via inclusion complexation with CD-NPs to form large nano assemblies. Then, the included or captured C60 can be released via the addition of an inclusion compotator as adamantane molecules, as illustrated in<sup>270</sup> The reversibility of the modified smart system can be utilized also for the fabrication and designing of other functional supramolecular hybrid materials.<sup>270</sup> Similarly, a water-soluble nanoaggregate was constructed via the inclusion complexation between fullerene and  $\alpha$ -CD.<sup>271</sup>

Cyclodextrins can include linear polymers such as PEG and PPG to form CD-capped poly-rotaxanes, with specific lengths depending on the utilized polymers’ molecular weight.<sup>272</sup> There are various poly-pseudo-rotaxanes formulated from threading either native  $\beta$ -CD or L-tryptophan-modified  $\beta$ -CD onto the amino-terminated PPG chains of different Mwt or lengths.<sup>273</sup> Afterward, further assembling of the modified polysiloxanes with AuNPs leads to the construction of different supramolecular networks. The modified hydrophilic aggregates or networks were characterized using different analyses including UV spectroscopy, FT-IR, X-ray diffraction <sup>1</sup>H NMR, TEM, and fluorescence spectroscopy.

The mechanism of polyurethane adsorption on the surfaces of AuNPs was carried out via the electrostatic interaction between the amino groups end capping polyrotaxanes and AuNPs. The results indicated that the sedimentation rate and the modified gold aggregates’ size mainly depended on the PPG chain lengths.<sup>273</sup>

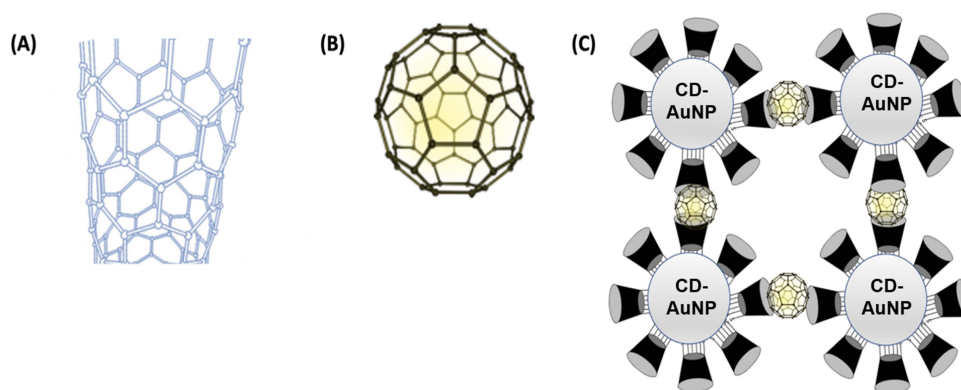


**Figure 11** Schematic illustration of Fullerene tube or cylindrical structure (A), ball-like structure (B), and the formation of water-soluble nanoaggregates via the inclusion complexation between Fullerene and  $\gamma$ -CD-decorating AuNPs (C).

Interestingly, the modified Au-aggregates, involving many L-tryptophan moieties, have both water solubility. In addition, the modified system has the ability for capturing or loading of fullerene (C60 analog) in water solution (ie, improve the aqueous solubility of fullerenes). Moreover, the obtained nano assemblies loaded with fullerene exhibited not only water solubility but also a high ability for DNA cleavage under light irradiation, which can be a promising system having potential applications in material and biological science.<sup>273</sup>

## Conclusion

Due to its wide range of applications, nanotechnology is a promising and growing medical research area. AuNPs possess targeted drug delivery with low toxicity and ease of detection. Higher stability and drug loading compared with microparticles and liposomes. Cyclodextrins and their derivatives gain a great interest from researchers in the last decade due to their role in enhancing drug solubility and stability via the inclusion of complexation with hydrophobic moieties. In our article, we tried to highlight the chemistry and application of different cyclodextrins, especially the ability of inclusion complexes formation. Also, it focuses deeply on cyclodextrin's role in improving drug loading capacity, stability, and size control of gold NPs. Moreover, in our review, we presented the reported roles of CDs in the design and applications of CD-conjugating gold nanoparticles (CD-AuNPs) in different biomedical fields, including drug delivery, antimicrobial, anticancer, and gene delivery and various targeted drug and gene delivery, preparation and improvement of catalytic enzymes, formation of self-assembling molecular print boards, and the fabrication of supra-molecular functionalized electrodes and biosensors formation. Also, this review focused on applying nano-aggregates to separate fullerenes in an aqueous medium. The present review realized that the nano-systems composed of AuNPs-CD are very promising and open the door for further pharmaceutical and biomedical applications.

## Acknowledgments

The authors extend their appreciation to the Deputyship for Research & Innovation, Ministry of Education, Saudi Arabia, for funding this research work through project number (QU-IF-1-2-1). The authors also thank Qassim University for its technical support.

## Disclosure

The authors declare that there are no conflicts of interest.

## References

1. Villiers A. Sur la fermentation de la fécule par l'action du ferment butyrique. *Compt Rend Acad Sci.* 1891;112:536–538.
2. D'Aria F, Pagano B, Giancola C. Thermodynamic properties of hydroxypropyl- $\beta$ -cyclodextrin/guest interaction: a survey of recent studies. *J Therm Anal Calorim.* 2022;147(8):4889–4897. doi:10.1007/s10973-021-10958-1
3. Saenger W. Cyclodextrin inclusion compounds in research and industry. *Angew Chemie Int Ed English.* 1980;19(5):344–362.
4. Tian B, Xiao D, Hei T, Ping R, Hua S, Liu J. The application and prospects of cyclodextrin inclusion complexes and polymers in the food industry: a review. *Polym Int.* 2020;69(7):597–603. doi:10.1002/pi.5992
5. Endo T, Nagase H, Ueda H, Shigihara A, Kobayashi S, Nagai T. Isolation, purification, and characterization of Cyclomaltooctadecaose ( $\nu$ -Cyclodextrin), Cyclomaltononadecaose ( $\xi$ -Cyclodextrin), Cyclomaltoeicosaose ( $\sigma$ -Cyclodextrin) and Cyclomaltoheicosaose ( $\pi$ -Cyclodextrin). *Chem Pharm Bull.* 1998;46(11):1840–1843.
6. Rowe RC, Sheskey P, Quinn M. *Handbook of Pharmaceutical Excipients.* Libros Digitales-Pharmaceutical Press; 2009.
7. Morin-Crini N, Fourmentin S, Fenyvesi E, et al. *130 Years of Cyclodextrin Discovery for Health, Food, Agriculture, and the Industry: A Review.* Vol. 19. Springer International Publishing; 2021. doi:10.1007/s10311-020-01156-w
8. Liu Z, Ye L, Xi J, Wang J. Cyclodextrin polymers: structure, synthesis, and use as drug carriers. *Prog Polym Sci.* 2021;118:101408. doi:10.1016/j.progpolymsci.2021.101408
9. Del Valle EMM. Cyclodextrins and their uses: a review. *Process Biochem.* 2004;39(9):1033–1046. doi:10.1016/S0032-9592(03)00258-9
10. Loftsson T, Duchene D. Cyclodextrins and their pharmaceutical applications. *Int J Pharm.* 2007;329(1–2):1–11. doi:10.1016/j.ijpharm.2006.07.009
11. Qi Z, Sikorski CT. Controlled delivery using cyclodextrin technology. *Pharm Tech Eur.* 1999;13(11):17–20.
12. Almawash S, El Hamd MA, Osman SK. Polymerized  $\beta$ -Cyclodextrin-based injectable hydrogel for sustained release of 5-Fluorouracil/Methotrexate mixture in breast cancer management: in vitro and In vivo analytical validations. *Pharmaceutics.* 2022;14(4):4. doi:10.3390/pharmaceutics14040817
13. Gidwani B, Vyas A. A Comprehensive review on cyclodextrin-based carriers for delivery of chemotherapeutic cytotoxic anticancer drugs. *Biomed Res Int.* 2015;2015:675. doi:10.1155/2015/198268

14. Kim Y. Inclusion complexation of ziprasidone mesylate with  $\beta$ -cyclodextrin sulfoethyl ether. *J Pharm Sci.* 1998;87(12):1560–1567. doi:10.1021/js980109t
15. Pandey A. Cyclodextrin-based nanoparticles for pharmaceutical applications: a review. *Environ Chem Lett.* 2021;19(6):4297–4310. doi:10.1007/s10311-021-01275-y
16. Szejtli J. Introduction and general overview of cyclodextrin chemistry. *Chem Rev.* 1998;98(5):1743–1753. doi:10.1002/chin.199839312
17. Abdulaziz F, Salah D. Gold nanoparticles incorporated with cyclodextrins and its applications. *J Biomater Nanobiotechnol.* 2021;12(04):79–97. doi:10.4236/jbnt.2021.124007
18. Higuchi T, Connor KA. A phase solubility technique. *Adv Anal Chem Instrum.* 1965;4:117–211.
19. Paczkowska M, Szymanowska-Powalowska D, Mizera M, et al. Cyclodextrins as multifunctional excipients: influence of inclusion into  $\beta$ -cyclodextrin on physicochemical and biological properties of tebipenem pivoxil. *PLoS One.* 2019;14(1):1–22. doi:10.1371/journal.pone.0210694
20. Challa R, Ahuja A, Ali J, Khar RK. Cyclodextrins in drug delivery: an updated review. *Aaps Pharmscitech.* 2005;6(2):E329–E357.
21. Osman SK, Soliman GM, Abd El Rasoul S. Physically cross-linked hydrogels of beta-cyclodextrin polymer and poly(ethylene glycol)-cholesterol as delivery systems for macromolecules and small drug molecules. *Curr Drug Deliv.* 2015;12:415–424.
22. Rajbanshi B, Saha S, Das K, et al. Study to probe subsistence of host-guest inclusion complexes of  $\alpha$  and  $\beta$ -cyclodextrins with biologically potent drugs for safety regulatory discharge. *Sci Rep.* 2018;8(1):1–20. doi:10.1038/s41598-018-31373-x
23. Osman SK, Brandl FP, Zayed GM, Teßmar JK, Göpferich AM. Cyclodextrin based hydrogels: inclusion complex formation and micellization of adamantane and cholesterol grafted polymers. *Polymer (Guildf).* 2011;52(21):4806–4812. doi:10.1016/j.polymer.2011.07.059
24. Mohammad A, Singh S, Swain S. Cyclodextrins: concept to applications, regulatory issues and challenges. *Nanomedicine Res J.* 2020;5(3):202–214. doi:10.22034/NMRJ.2020.03.001
25. Saokham P, Muangkaew C, Jansook P, Loftsson T. Solubility of cyclodextrins and drug/cyclodextrin complexes. *Molecules.* 2018;23(5):1–15. doi:10.3390/molecules23051161
26. Tomasik P, Schilling CH. Complexes of starch with organic guests. *Adv Carbohydr Chem Biochem.* 1998;53:263–343. doi:10.1016/s0065-2318(08)60047-5
27. Marques CS, Carvalho SG, Bertoli LD, et al.  $\beta$ -Cyclodextrin inclusion complexes with essential oils: obtention, characterization, antimicrobial activity and potential application for food preservative sachets. *Food Res Int.* 2019;119:(January):499–509. doi:10.1016/j.foodres.2019.01.016
28. Dora CP, Trotta F, Kushwah V, et al. Potential of erlotinib cyclodextrin nanosponge complex to enhance solubility, dissolution rate, in vitro cytotoxicity and oral bioavailability. *Carbohydr Polym.* 2016;137:339–349. doi:10.1016/j.carbpol.2015.10.080
29. Bilensoy E, Çırpanlı Y, Şen M, Doğan AL, Çalış S. Thermosensitive mucoadhesive gel formulation loaded with 5-Fu: cyclodextrin complex for HPV-induced cervical cancer. *J Incl Phenom Macrocycl Chem.* 2007;57(1–4):363–370. doi:10.1007/s10847-006-9259-y
30. Loftsson T, Jarho P, Másson M, Järvinen T. Cyclodextrins in drug delivery. *Expert Opin Drug Deliv.* 2005;2(2):335–351. doi:10.1517/17425247.2.1.335
31. Gadade DD, Pekamwar SS. Cyclodextrin based nanoparticles for drug delivery and theranostics. *Adv Pharm Bull.* 2020;10(2):166–183. doi:10.34172/apb.2020.022
32. Davis ME, Brewster ME. Cyclodextrin-based pharmaceuticals: past, present and future. *Nat Rev Drug Discov.* 2004;3(12):1023–1035. doi:10.1038/nrd1576
33. Crini G, Fourmentin S, Fenyvesi É, Torri G, Fourmentin M, Morin-Crini N. Cyclodextrins, from molecules to applications. *Environ Chem Lett.* 2018;16(4):1361–1375. doi:10.1007/s10311-018-0763-2
34. Liu Y, Chen Y, Gao X, Fu J, Hu L. Application of cyclodextrin in food industry. *Crit Rev Food Sci Nutr.* 2020;62(10):2627–2640. doi:10.1080/10408398.2020.1856035
35. Matencio A, Hoti G, Monfared YK, et al. Cyclodextrin monomers and polymers for drug activity enhancement. *Polymers (Basel).* 2021;13(11):1–18. doi:10.3390/polym13111684
36. Petitjean M, García-Zubiri IX, Isasi JR. History of cyclodextrin-based polymers in food and pharmacy: a review. *Environ Chem Lett.* 2021;19(4):3465–3476. doi:10.1007/s10311-021-01244-5
37. Yuan Z, Liu H, Wu H, et al. Cyclodextrin Hydrogels: rapid Removal of Aromatic Micropollutants and Adsorption Mechanisms. *J Chem Eng Data.* 2020;65(2):678–689. doi:10.1021/acs.jced.9b00913
38. Malik NS, Ahmad M, Alqahtani MS, et al.  $\beta$ -cyclodextrin chitosan-based hydrogels with tunable pH-responsive properties for controlled release of Acyclovir: design, characterization, safety, and pharmacokinetic evaluation. *Drug Deliv.* 2021;28(1):1093–1108. doi:10.1080/10717544.2021.1921074
39. Hong W, Guo F, Yu N, et al. A novel folic acid receptor-targeted drug delivery system based on curcumin-loaded  $\beta$ -cyclodextrin nanoparticles for cancer treatment. *Drug Des Devel Ther.* 2021;15:(May):2843–2855. doi:10.2147/DDDT.S320119
40. Xu W, Li X, Wang L, et al. Design of cyclodextrin-based functional systems for biomedical applications. *Front Chem.* 2021;9:(February):1–13. doi:10.3389/fchem.2021.635507
41. Balaji A, Pandey VP, Srinath MS, Manavalan R. Synthesis and characterization studies of cisplatin/hydroxypropyl- $\beta$ -cyclodextrin complex. *Pharmacologyonline.* 2009;1:1135–1143.
42. Zhang L, Man S, Qiu H, et al. Curcumin-cyclodextrin complexes enhanced the anti-cancer effects of curcumin. *Environ Toxicol Pharmacol.* 2016;48:31–38. doi:10.1016/j.etap.2016.09.021
43. Nanda A, Sahoo RN, Pramanik A, et al. Drug-in-mucoadhesive type film for ocular anti-inflammatory potential of amlodipine: effect of sulphobutyl-ether-beta-cyclodextrin on permeation and molecular docking characterization. *Colloids Surfaces B Biointerfaces.* 2018;172:(August):555–564. doi:10.1016/j.colsurfb.2018.09.011
44. Vieira da Silva SA, Clemente A, Rocha J, et al. Anti-inflammatory effect of limonin from cyclodextrin (un)processed Orange juices in vivo acute inflammation and chronic rheumatoid arthritis models. *J Funct Foods.* 2018;49(August):146–153. doi:10.1016/j.jff.2018.08.024
45. Ling W, Xuehua J, Weijuan X, Chenrui L. Complexation of tanshinone IIA with 2-hydroxypropyl- $\beta$ -cyclodextrin: effect on aqueous solubility, dissolution rate, and intestinal absorption behavior in rats. *Int J Pharm.* 2007;341(1–2):58–67. doi:10.1016/j.ijpharm.2007.03.046

46. Wu Y, Xiao Y, Yue Y, Zhong K, Zhao Y, Gao H. A deep insight into mechanism for inclusion of 2R,3R-dihydromyricetin with cyclodextrins and the effect of complexation on antioxidant and lipid-lowering activities. *Food Hydrocoll.* 2020;103:105718. doi:10.1016/j.foodhyd.2020.105718
47. Lahiani-Skiba M, Bounoure F, Fessi H, Skiba M. Effect of cyclodextrins on lonidamine release and in-vitro cytotoxicity. *J Incl Phenom Macrocycl Chem.* 2011;69(3–4):481–485. doi:10.1007/s10847-010-9872-7
48. Jacob S, Nair AB. Cyclodextrin complexes: perspective from drug delivery and formulation. *Drug Dev Res.* 2018;79(5):201–217. doi:10.1002/ddr.21452
49. Mura P. Analytical techniques for characterization of cyclodextrin complexes in the solid state: a review. *J Pharm Biomed Anal.* 2015;113:226–238. doi:10.1016/j.jpba.2015.01.058
50. Mura P, Adragna E, Rabasco AM, et al. Effects of the host cavity size and the preparation method on the physicochemical properties of ibuprofen-cyclodextrin systems. *Drug Dev Ind Pharm.* 1999;25(3):279–287.
51. Mura P, Faucci MT, Parrini PL, Furlanetto S, Pinzauti S. Influence of the preparation method on the physicochemical properties of ketoprofen-cyclodextrin binary systems. *Int J Pharm.* 1999;179(1):117–128.
52. Allahyari S, Trotta F, Valizadeh H, Jelvehgari M, Zakeri-Milani P. Cyclodextrin based nanosponges as promising carriers for active agents. *Expert Opin Drug Deliv.* 2019;16(5):467–479. doi:10.1080/17425247.2019.1591365
53. Tannous M, Caldera F, Hoti G, Dianzani U, Cavalli R, Trotta F. Drug-encapsulated cyclodextrin nanosponges. In: *supramolecules in Drug Discovery and Drug Delivery: methods and Protocols. Methods in Molecular Biology.* 2021;2207. doi:10.1007/978-1-0716-0920-0
54. Sadaquat H, Akhtar M. Comparative effects of  $\beta$ -cyclodextrin, HP- $\beta$ -cyclodextrin and SBE7- $\beta$ -cyclodextrin on the solubility and dissolution of docetaxel via inclusion complexation. *J Incl Phenom Macrocycl Chem.* 2020;96(3–4):333–351. doi:10.1007/s10847-020-00977-0
55. Zia V, Rajewski RA, Stella VJ. Effect of cyclodextrin charge on complexation of neutral and charged substrates: comparison of (SBE)7m- $\beta$ -CD to HP- $\beta$ -CD. *Pharm Res.* 2001;18(5):667–673. doi:10.1023/A:
56. Nagase Y, Hirata M, Wada K, et al. Improvement of some pharmaceutical properties of DY-9760e by sulfobutyl ether  $\beta$ -cyclodextrin. *Int J Pharm.* 2001;229:163–172. doi:10.1007/s10847-010-9870-9
57. Tros de Iarduya MC, Martín C, Goñi MM, Martínez-Ohárriz MC. Solubilization and interaction of sulindac with  $\beta$ -cyclodextrin in the solid state and in aqueous solution. *Drug Dev Ind Pharm.* 1998;24(3):301–306. doi:10.3109/03639049809085624
58. Loftsson T, Brewster ME. Pharmaceutical applications of cyclodextrins. 1. Drug solubilization and stabilization. *J Pharm Sci.* 1996;85(10):1017–1025. doi:10.1021/js950534b
59. Dalmora MEA. Inclusion complex of piroxicam with  $\beta$ -cyclodextrin and incorporation in hexadecyltrimethylammonium bromide based microemulsion. *Int J Pharm.* 1999;184(2):184.
60. Cedillo-Flores OE, Rodríguez-Laguna N, Hipólito-Nájera AR, Nivón-Ramírez D, Gómez-Balderas R, Moya-Hernández R. Effect of the pH on the thermodynamic stability of inclusion complexes of thymol and carvacrol in  $\beta$ -cyclodextrin in water. *Food Hydrocoll.* 2022;124(March):2021. doi:10.1016/j.foodhyd.2021.107307
61. Yavuz B, Bilensoy E, Vural I, Şumnu M. Alternative oral exemestane formulation: improved dissolution and permeation. *Int J Pharm.* 2010;398(1–2):137–145. doi:10.1016/j.ijpharm.2010.07.046
62. Wadhwa G, Kumar S, Chhabra L, Mahant S, Rao R. Essential oil-cyclodextrin complexes: an updated review. *J Incl Phenom Macrocycl Chem.* 2017;89(1–2):39–58. doi:10.1007/s10847-017-0744-2
63. Jiang L, Yang J, Wang Q, Ren L, Zhou J. Physicochemical properties of catechin/ $\beta$ -cyclodextrin inclusion complex obtained via coprecipitation. *CYTA - J Food.* 2019;17(1):544–551. doi:10.1080/19476337.2019.1612948
64. Jug M, Mura PA. Grinding as solvent-free green chemistry approach for cyclodextrin inclusion complex preparation in the solid state. *Pharmaceutics.* 2018;10:4. doi:10.3390/pharmaceutics10040189
65. Banchemo M. Supercritical carbon dioxide as a green alternative to achieve drug complexation with cyclodextrins. *Pharmaceutics.* 2021;14:6. doi:10.3390/ph14060562
66. Kaur K, Jindal R, Jindal D. Synthesis, characterization and studies on host-guest interactions of inclusion complexes of metformin hydrochloride with  $\beta$ -cyclodextrin. *J Mol Liq.* 2019;282:162–168. doi:10.1016/j.molliq.2019.02.127
67. Khushbu JR. Cyclodextrin mediated controlled release of edaravone from pH-responsive sodium alginate and chitosan based nanocomposites. *Int J Biol Macromol.* 2022;202:(January):11–25. doi:10.1016/j.ijbiomac.2022.01.001
68. Al-Marzouqi AH, Elwy HM, Shehadi I, Adem A. Physicochemical properties of antifungal drug-cyclodextrin complexes prepared by supercritical carbon dioxide and by conventional techniques. *J Pharm Biomed Anal.* 2009;49(2):227–233. doi:10.1016/j.jpba.2008.10.032
69. Moyano JR, Arias MJ, Gines JM, Perez JI, Rabasco AM. Dissolution Behavior of Oxazepam in Presence of Cyclodextrins: evaluation of Oxazepam-Dimeb Binary System. *Drug Dev Ind Pharm.* 1997;23(4):379–385.
70. Li B, Li N, Wang S, Gao J, Fang S. Pharmacokinetics of injectable beta-Cyclodextrin-Oridonin inclusion complex, a novel formulation of oridonin in Wistar rats. *Natl J Physiol Pharm Pharmacol.* 2012;2(1):52–57.
71. Castillo JA, Palomo-Canales J, Garcia JJ, Lastres JL, Bolas F, Torrado JJ. Preparation and characterization of albendazole  $\beta$ -cyclodextrin complexes. *Drug Dev Ind Pharm.* 1999;25(12):1241–1248.
72. Cid-Samamed A, Rakmaï J, Mejuto JC, Simal-Gandara J, Astray G. Cyclodextrins inclusion complex: preparation methods, analytical techniques and food industry applications. *Food Chem.* 2022;384:132467. doi:10.1016/j.foodchem.2022.132467
73. Parlati S, Gobetto R, Barolo C, et al. Preparation and application of a  $\beta$ -cyclodextrin-disperse/reactive dye complex. *J Incl Phenom Macrocycl Chem.* 2007;57(1–4):463–470. doi:10.1007/s10847-006-9235-6
74. Pereva S, Sarafska T, Bogdanova S, Spassov T. Efficiency of “cyclodextrin-ibuprofen” inclusion complex formation. *J Drug Deliv Sci Technol.* 2016;35:34–39. doi:10.1016/j.jddst.2016.04.006
75. Ghorab MK, Adeyeye MC. Enhancement of ibuprofen dissolution via wet granulation with  $\beta$ -cyclodextrin. *Pharm Dev Technol.* 2001;6(3):305–314. doi:10.1081/PDT-100002611
76. Reddy MN, Rehana T, Ramakrishna S, Chowdary KPR, Diwan PV.  $\beta$ -cyclodextrin complexes of celecoxib: molecular-modeling, characterization, and dissolution studies. *AAPS J.* 2004;6(1):1–9. doi:10.1208/ps060107
77. Patel HM, Suhagia BN, Shah SA, Rathod IS, Parmar VK. Preparation and characterization of etoricoxib- $\beta$ -cyclodextrin complexes prepared by the kneading method. *Acta Pharm.* 2007;57(3):351–359. doi:10.2478/v10007-007-0028-2

78. Swami G, Koshy MK, Pandey M, Saraf SA. Preparation and characterization of domperidone- $\beta$ -cyclodextrin complexes prepared by kneading method. *Int J Adv Pharm Sci.* 2010;1(1):68–74. doi:10.5138/ijaps.2010.0976.1055.01008
79. Songkro S, Hayook N, Jaisawang J, Maneenuan D, Chuchome T, Kaewnopparat N. Investigation of inclusion complexes of citronella oil, citronellal and citronellol with  $\beta$ -cyclodextrin for mosquito repellent. *J Incl Phenom Macrocycl Chem.* 2012;72(3–4):339–355. doi:10.1007/s10847-011-9985-7
80. Pralhad T, Rajendrakumar K. Study of freeze-dried quercetin-cyclodextrin binary systems by DSC, FT-IR, X-ray diffraction and SEM analysis. *J Pharm Biomed Anal.* 2004;34(2):333–339. doi:10.1016/S0731-7085(03)00529-6
81. Villalonga R, Cao R, Fragoso A, Damiao AE, Ortiz PD, Caballero J. Supramolecular-mediated bienzymatic immobilization of catalase and superoxide dismutase on  $\beta$ -cyclodextrin-modified gold nanospheres. *J Mol Catal B Enzym.* 2005;35:79.
82. Li N, Wang N, Wu T, et al. Preparation of curcumin-hydroxypropyl- $\beta$ -cyclodextrin inclusion complex by cosolvency-lyophilization procedure to enhance oral bioavailability of the drug. *Drug Dev Ind Pharm.* 2018;44(12):1966–1974. doi:10.1080/03639045.2018.1505904
83. Elgindy N, Elkhodairy K, Molokhia A, Elzoghby A. Lyophilization monophasic solution technique for improvement of the physicochemical properties of an anticancer drug, flutamide. *Eur J Pharm Biopharm.* 2010;74(2):397–405. doi:10.1016/j.ejpb.2009.11.011
84. Eid EEM, Abdul AB, Suliman FEO, Sukari MA, Rasheed A, Fatah SS. Characterization of the inclusion complex of zerumbone with hydroxypropyl- $\beta$ -cyclodextrin. *Carbohydr Polym.* 2011;83(4):1707–1714. doi:10.1016/j.carbpol.2010.10.033
85. Ozdemir N, Pola CC, Teixeira BN, Hill LE, Bayrak A, Gomes CL. Preparation of black pepper oleoresin inclusion complexes based on beta-cyclodextrin for antioxidant and antimicrobial delivery applications using kneading and freeze drying methods: a comparative study. *Lwt-Food Sci Technol.* 2018;91:439–445. doi:10.1016/j.lwt.2018.01.046
86. Skalko-basnet N, Pavelic Z, Becirevic-lacan M. Liposomes containing drug and cyclodextrin prepared by the one-step spray-drying method. *Drug Dev Ind Pharm.* 2000;26(12):1279–1284.
87. Cabral-Marques H, Almeida R. Optimisation of spray-drying process variables for dry powder inhalation (DPI) formulations of corticosteroid/cyclodextrin inclusion complexes. *Eur J Pharm Biopharm.* 2009;73(1):121–129. doi:10.1016/j.ejpb.2009.05.002
88. Borghetti GS, Lula IS, Sinisterra RD, Bassani VL. Quercetin/ $\beta$ -Cyclodextrin solid complexes prepared in aqueous solution followed by spray-drying or by physical mixture. *AAPS PharmSciTech.* 2009;10(1):235–242. doi:10.1208/s12249-009-9196-3
89. Miletic T, Kyriakos K, Graovac A, Ibric S. Spray-dried voriconazole-cyclodextrin complexes: solubility, dissolution rate and chemical stability. *Carbohydr Polym.* 2013;98(1):122–131. doi:10.1016/j.carbpol.2013.05.084
90. Watson MA, Lea JM, Bett-Garber KL. Spray drying of pomegranate juice using maltodextrin/cyclodextrin blends as the wall material. *Food Sci Nutr.* 2017;5(3):820–826. doi:10.1002/fsn3.467
91. Ramos AI, Braga TM, Silva P, et al. Chloramphenicol-cyclodextrin inclusion compounds: co-dissolution and mechanochemical preparations and antibacterial action. *CrystEngComm.* 2013;15(15):2822–2834. doi:10.1039/c3ce26414a
92. Mura P, Fauci MT, Maestrelli F, Furlanetto S, Pinzauti S. Characterization of physicochemical properties of naproxen systems with amorphous  $\beta$ -cyclodextrin-epichlorohydrin polymers. *J Pharm Biomed Anal.* 2002;29(6):1015–1024. doi:10.1016/S0731-7085(02)00142-5
93. Tan Q, He D, Wu M, et al. Characterization, activity, and computer modeling of a molecular inclusion complex containing rifaldazine. *Int J Nanomedicine.* 2013;8:477–484. doi:10.2147/IJN.S38937
94. He D, Deng P, Yang L, et al. Molecular encapsulation of rifampicin as an inclusion complex of hydroxypropyl- $\beta$ -cyclodextrin: design, characterization and in vitro dissolution. *Colloids Surfaces B Biointerfaces.* 2013;103:580–585. doi:10.1016/j.colsurfb.2012.10.062
95. Cugovčan M, Jablan J, Lovrić J, Cinčić D, Galić N, Jug M. Biopharmaceutical characterization of praziquantel cocrystals and cyclodextrin complexes prepared by grinding. *J Pharm Biomed Anal.* 2017;137:42–53. doi:10.1016/j.jpba.2017.01.025
96. Ali HRH, Saleem IY, Tawfeek HM. Insight into inclusion complexation of indomethacin nicotinamide cocrystals. *J Incl Phenom Macrocycl Chem.* 2016;84(3–4):179–188. doi:10.1007/s10847-016-0594-3
97. Jug M, Mennini N, Kóvér KE, Mura P. Comparative analysis of binary and ternary cyclodextrin complexes with econazole nitrate in solution and in solid state. *J Pharm Biomed Anal.* 2014;91:81–91. doi:10.1016/j.jpba.2013.12.029
98. Majewska K, Skwierawska A, Kamińska B, Przeźniak-Welenc M. Improvement of oipramol base solubility by complexation with  $\beta$ -cyclodextrin. *Supramol Chem.* 2018;30(1):20–31. doi:10.1080/10610278.2017.1350677
99. Malaquias LFB, Sá-Barreto LCL, Freire DO, et al. Taste masking and rheology improvement of drug complexed with beta-cyclodextrin and hydroxypropyl- $\beta$ -cyclodextrin by hot-melt extrusion. *Carbohydr Polym.* 2018;185:19–26. doi:10.1016/j.carbpol.2018.01.011
100. Conceição J, Farto-Vaamonde X, Goyanes A, et al. Hydroxypropyl- $\beta$ -cyclodextrin-based fast dissolving carbamazepine printlets prepared by semisolid extrusion 3D printing. *Carbohydr Polym.* 2019;221:55–62. doi:10.1016/j.carbpol.2019.05.084
101. Granados PA, Pinho LAG, Sa-Barreto LL, Gratieri T, Gelfuso GM, Cunha-Filho M. Application of hot-melt extrusion in the complexation of naringenin with cyclodextrin using hydrophilic polymers. *Adv Powder Technol.* 2022;33(1):103380. doi:10.1016/j.apt.2021.11.032
102. Saucéau M, Rodier E, Fages J. Preparation of inclusion complex of piroxicam with cyclodextrin by using supercritical carbon dioxide. *J Supercrit Fluids.* 2008;47(2):326–332. doi:10.1016/j.supflu.2008.07.006
103. Banhero M, Ronchetti S, Manna L. Characterization of ketoprofen/methyl- $\beta$ -cyclodextrin complexes prepared using supercritical carbon dioxide. *J Chem.* 2013;2013:45. doi:10.1155/2013/583952
104. Hussein K, Türk M, Wahl MA. Comparative evaluation of Ibuprofen/ $\beta$ -cyclodextrin complexes obtained by supercritical carbon dioxide and other conventional methods. *Pharm Res.* 2007;24(3):585–592. doi:10.1007/s11095-006-9177-0
105. Al-Marzouqi AH, Jobe B, Dowaidar A, Maestrelli F, Mura P. Evaluation of supercritical fluid technology as preparative technique of benzocaine-cyclodextrin complexes-Comparison with conventional methods. *J Pharm Biomed Anal.* 2007;43(2):566–574. doi:10.1016/j.jpba.2006.08.019
106. Al-Marzouqi A, Jobe B, Corti G, Cirri M, Mura P. Physicochemical characterization of drug-cyclodextrin complexes prepared by supercritical carbon dioxide and by conventional techniques. *J Incl Phenom Macrocycl Chem.* 2007;57(1–4):223–231. doi:10.1007/s10847-006-9192-0
107. Al-Marzouqi AH, Solieman A, Shehadi I, Adem A. Influence of the preparation method on the physicochemical properties of econazole- $\beta$ -cyclodextrin complexes. *J Incl Phenom Macrocycl Chem.* 2008;60(1–2):85–93. doi:10.1007/s10847-007-9356-6
108. Rudrangi SRS, Trivedi V, Mitchell JC, Wicks SR, Alexander BD. Preparation of olanzapine and methyl- $\beta$ -cyclodextrin complexes using a single-step, organic solvent-free supercritical fluid process: an approach to enhance the solubility and dissolution properties. *Int J Pharm.* 2015;494(1):408–416. doi:10.1016/j.ijpharm.2015.08.062

109. Mohammed AM, Faisal W, Saleh KI, Osman SK. Aqueous solubility and dissolution rate improvement of etodolac via inclusion complexation technique. *Int J Pharmacol Pharm Res Hum Journals*. 2016;6(3):304–318.
110. Adeoye O, Costa C, Casimiro T, Aguiar-Ricardo A, Cabral-Marques H. Preparation of ibuprofen/hydroxypropyl- $\beta$ -cyclodextrin inclusion complexes using supercritical CO<sub>2</sub>-assisted spray drying. *J Supercrit Fluids*. 2018;133:479–485. doi:10.1016/j.supflu.2017.11.009
111. Ling XY, Malaquin L, Reinhoudt DN, Wolf H, Huskens J. An in situ study of the adsorption behavior of functionalized particles on self-assembled monolayers via different chemical interactions. *Langmuir*. 2007;23(20):9990–9999. doi:10.1021/la701671s
112. Maestrelli F, González-Rodríguez ML, Rabasco AM, Mura P. Preparation and characterisation of liposomes encapsulating ketoprofen-cyclodextrin complexes for transdermal drug delivery. *Int J Pharm*. 2005;298(1):55–67. doi:10.1016/j.ijpharm.2005.03.033
113. Veiga F, Fernandes C, Maincent P. Influence of the preparation method on the physicochemical properties of tolbutamide/cyclodextrin binary systems. *Drug Dev Ind Pharm*. 2001;27(6):523–532. doi:10.1081/DDC-100105177
114. Shan-Yang L, Yuh-Horng K. Solid particulates of drug- $\beta$ -cyclodextrin inclusion complexes directly prepared by a spray-drying technique. *Int J Pharm*. 1989;56(3):249–259. doi:10.1016/0378-5173(89)90022-7
115. Yang X, Shen J, Liu J, et al. Spray-drying of hydroxypropyl  $\beta$ -cyclodextrin microcapsules for co-encapsulation of resveratrol and piperine with enhanced solubility. *Crystals*. 2022;12:5. doi:10.3390/cryst12050596
116. Gao X, Chen G, Ning L. Plasmonic characteristics of nanorod-based metallic nanostructures. *Opt Laser Technol*. 2013;48:394–400. doi:10.1016/j.optlastec.2012.10.036
117. Wanunu M, Popovitz-Biro R, Cohen H, Vaskevich A, Rubinstein I. Coordination-based gold nanoparticle layers. *J Am Chem Soc*. 2005;127(25):9207–9215. doi:10.1021/ja050016v
118. Barrientos L, Yutronic N, Del monte F, Gutiérrez MC, Jara P. Ordered arrangement of gold nanoparticles on an  $\alpha$ -cyclodextrin-dodecanethiol inclusion compound produced by magnetron sputtering. *New J Chem*. 2007;31(8):1400–1402. doi:10.1039/b706346f
119. Dreaden EC, Alkilany AM, Huang X, Murphy CJ, El-Sayed MA. The golden age: gold nanoparticles for biomedicine. *Chem Soc Rev*. 2012;41(7):2740–2779. doi:10.1039/c1cs15237h
120. Liu Y, Male KB, Bouvrette P, Luong JHT. Control of the size and distribution of gold nanoparticles by unmodified cyclodextrins. *Chem Mater*. 2003;15(22):4172–4180. doi:10.1021/cm0342041
121. Nie S, Xing Y, Kim GJ, Simons JW. Nanotechnology applications in cancer. *Annu Rev Biomed Eng*. 2007;9:257–288. doi:10.1146/annurev.bioeng.9.060906.152025
122. Wang MD, Shin DM, Simons JW, Nie S. Nanotechnology for targeted cancer therapy. *Expert Rev Anticancer Ther*. 2007;7(6):833–837. doi:10.1586/14737140.7.6.833
123. You -C-C, Miranda OR, Gider B, et al. Detection and identification of proteins using nanoparticle-fluorescent polymer “chemical nose” sensors. *Nat Nanotechnol*. 2007;2(5):318–323. doi:10.1038/nnano.2007.99
124. Bhattacharya R, Patra CR, Earl A, et al. Attaching folic acid on gold nanoparticles using noncovalent interaction via different polyethylene glycol backbones and targeting of cancer cells. *Nanomed Nanotechnol Biol Med*. 2007;3(3):224–238. doi:10.1016/j.nano.2007.07.001
125. Li J, Lou Z. Synthesis and applications of gold nanoparticles. *Pharmacologyonline*. 2021;3:1870–1874. doi:10.47583/ijpsrr.2022.v77i01.003
126. Faraday M. The Bakerian Lecture: experimental relations of gold (and other metals) to light. *Philos Trans R Soc London*. 1857;147:145–181. doi:10.1098/rstl.1857.0011
127. Turkevich J, Stevenson PC, Hillier J. A study of the nucleation and growth processes in the synthesis of colloidal gold. *Discuss Faraday Soc*. 1951;11(c):55–75. doi:10.1039/DF9511100055
128. Hayat MA. *Colloidal Gold: Principles, Methods, and Applications*. Elsevier; 2012.
129. Frens G. Controlled nucleation for the regulation of the particle size in monodisperse gold suspensions. *Nat Phys Sci*. 1973;241(105):20–22.
130. Zhao L, Jiang D, Cai Y, Ji X, Xie R, Yang W. Tuning the size of gold nanoparticles in the citrate reduction by chloride ions. *Nanoscale*. 2012;4(16):5071–5076. doi:10.1039/c2nr30957b
131. Shah M, Badwaik V, Kherde Y, et al. Gold nanoparticles : various methods of synthesis and antibacterial applications. *Front Biosci*. 2014;19:1320–1344.
132. Esumi K, Matsuhsa K, Torigoe K. Preparation of rodlike gold particles by UV irradiation using cationic micelles as a template. *Langmuir*. 1995;11:3285–3287.
133. Valden M, Lai X, Goodman DW. Onset of catalytic activity of gold clusters on titania with the appearance of nonmetallic properties. *Science*. 1998;281(5383):1647–1650.
134. Veith GM, Lupini AR, Pennycook SJ, Ownby GW, Dudney NJ. Nanoparticles of gold on  $\gamma$ -Al<sub>2</sub>O<sub>3</sub> produced by dc magnetron sputtering. *J Catal*. 2005;231(1):151–158. doi:10.1016/j.jcat.2004.12.008
135. Kabashin AV, Meunier M, Kingston C, Luong JHT. Fabrication and characterization of gold nanoparticles by femtosecond laser ablation in an aqueous solution of cyclodextrins. *J Phys Chem B*. 2003;107(19):4527–4531. doi:10.1021/jp034345q
136. Usman AI, Abdul Aziz A, Abu Noqta O. Application of green synthesis of gold nanoparticles: a review. *J Teknol*. 2017;79(5):1–5. doi:10.11113/jt.v81.11409
137. Santhosh PB, Julia Genova HC. Green synthesis of gold nanoparticles: an eco-friendly approach. *Chemistry*. 2015;4:345–369. doi:10.3390/chemistry4020026
138. Teimuri-Mofrad R, Hadi R, Tahmasebi B, Farhoudian S, Mehravar M, Nasiri R. Green synthesis of gold nanoparticles using plant extract: mini-review. *Nanochemistry Res*. 2017;2(1):8–19. doi:10.22036/ncr.2017.01.002
139. Kumar S, Gandhi KS, Kumar R. Modeling of formation of gold nanoparticles by citrate method. *Ind Eng Chem Res*. 2007;46(10):3128–3136. doi:10.1021/ie060672j
140. Sivaraman SK, Kumar S, Santhanam V. Monodisperse sub-10 nm gold nanoparticles by reversing the order of addition in Turkevich method – the role of chloroauric acid. *J Colloid Interface Sci*. 2011;361(2):543–547. doi:10.1016/j.jcis.2011.06.015
141. Ojea-Jiménez I, Romero FM, Bastús NG, Puentes V. Small gold nanoparticles synthesized with sodium citrate and heavy water: insights into the reaction mechanism. *J Phys Chem C*. 2010;114(4):1800–1804. doi:10.1021/jp9091305
142. Merza KS, Al-Attabi HD, Abbas ZM, Yusr HA. Comparative study on methods for preparation of gold nanoparticles. *Green Sustain Chem*. 2012;2(1):26–28. doi:10.4236/gsc.2012.21005

143. Waters CA, Mills AJ, Johnson KA, Schiffrin DJ. Purification of dodecanethiol derivatised gold nanoparticles. *Chem Commun.* 2003;3(4):540–541. doi:10.1039/b211874b
144. Luty-blocho M, Fitzner K, Hessel V, Löb P, Maskos M, Metzke D. Synthesis of gold nanoparticles in an interdigital micromixer using ascorbic acid and sodium borohydride as reducers. *Chem Eng.* 2011;171:279–290. doi:10.1016/j.cej.2011.03.104
145. Xu Z-C, Shen C-M, Xiao C-W, et al. Wet chemical synthesis of gold nanoparticles using silver seeds: a shape control from nanorods to hollow spherical nanoparticles. *Nanotechnology.* 2007;18(11):115608. doi:10.1088/0957-4484/18/11/115608
146. Shao L, Susha AS, Cheung LS, Sau TK, Rogach AL, Wang J. Plasmonic properties of single multispliked gold nanostars: correlating modeling with experiments. *Langmuir.* 2012;28(24):8979–8984. doi:10.1021/la2048097
147. Sau TK, Rogach AL, Döblinger M, Feldmann J. One-step high-yield aqueous synthesis of size-tunable multispliked gold nanoparticles. *Small.* 2011;7(15):2188–2194. doi:10.1002/sml.201100365
148. Prasad BLV, Stoeva SI, Sorensen CM, Klabunde KJ. Digestive ripening of thiolated gold nanoparticles: the effect of alkyl chain length. *Langmuir.* 2002;18:7515–7520.
149. John MG, Tibbetts KM. One-step femtosecond laser ablation synthesis of sub-3 nm gold nanoparticles stabilized by silica. *Appl Surf Sci.* 2019;475:1048–1057. doi:10.1016/j.apsusc.2019.01.042
150. Gingery D, Bühlmann P. Formation of gold nanoparticles on multiwalled carbon nanotubes by thermal evaporation. *Carbon N Y.* 2008;46(14):1966–1972. doi:10.1016/j.carbon.2008.08.007
151. Gaspar D, Pimentel AC, Mateus T, et al. Influence of the layer thickness in plasmonic gold nanoparticles produced by thermal evaporation. *Sci Rep.* 2013;3:1469. doi:10.1038/srep01469
152. Aswathy B, Avadhani GS, Suji S, Sony G. Synthesis of  $\beta$ -cyclodextrin functionalized gold nanoparticles for the selective detection of Pb<sup>2+</sup> ions from aqueous solution. *Front Mater Sci.* 2012;6(2):168–175. doi:10.1007/s11706-012-0165-5
153. George JM, Mathew B. Cyclodextrin-mediated gold nanoparticles as multisensing probe for the selective detection of hydroxychloroquine drug. *Korean J Chem Eng.* 2021;38(3):624–634. doi:10.1007/s11814-020-0719-7
154. Philip D. Honey mediated green synthesis of gold nanoparticles. *Spectrochim Acta.* 2009;73(4):650–653. doi:10.1016/j.saa.2009.03.007
155. Cherian T, Maity D, Kumar R, et al. Green chemistry based gold nanoparticles synthesis using the marine bacterium *Lysinibacillus odysssei* PBCW2 and their multitudinous activities. *Nanomaterials.* 2022;12(17):ye6. doi:10.3390/nano12172940
156. Zhang X, Qu Y, Shen W, et al. Biogenic synthesis of gold nanoparticles by yeast *Magnusiomyces ingens* LH-F1 for catalytic reduction of nitrophenols. *Colloids Surfaces a Physicochem Eng Asp.* 2016;497:280–285. doi:10.1016/j.colsurfa.2016.02.033
157. Molnár Z, Bódai V, Szakacs G, et al. Green synthesis of gold nanoparticles by thermophilic filamentous fungi. *Sci Rep.* 2018;8(1):1–12. doi:10.1038/s41598-018-22112-3
158. Ramakrishna M, Rajesh Babu D, Gengan RM, Chandra S, Nageswara Rao G. Green synthesis of gold nanoparticles using marine algae and evaluation of their catalytic activity. *J Nanostructure Chem.* 2016;6(1):1–13. doi:10.1007/s40097-015-0173-y
159. Colin JA, Pech-Pech IE, Oviedo M, Águila SA, Romo-Herrera JM, Contreras OE. Gold nanoparticles synthesis assisted by marine algae extract: biomolecules shells from a green chemistry approach. *Chem Phys Lett.* 2018;708:(August):210–215. doi:10.1016/j.cplett.2018.08.022
160. Sadeghi B, Mohammadzadeh M, Babakhani B. Green synthesis of gold nanoparticles using *Stevia rebaudiana* leaf extracts: characterization and their stability. *J Photochem Photobiol B Biol.* 2015;148:101–106. doi:10.1016/j.jphotobiol.2015.03.025
161. Awad MA, Eisa NE, Virk P, et al. Green synthesis of gold nanoparticles: preparation, characterization, cytotoxicity, and anti-bacterial activities. *Mater Lett.* 2019;256:126608. doi:10.1016/j.matlet.2019.126608
162. Bhattacharya R, Mukherjee P. Biological properties of “naked” metal nanoparticles. *Adv Drug Deliv Rev.* 2008;60(11):1289–1306. doi:10.1016/j.addr.2008.03.013
163. Burda C, Chen X, Narayanan R, El-Sayed MA. Chemistry and properties of nanocrystals of different shapes. *Chem Rev.* 2005;105(4):1025–1102. doi:10.1021/cr030063a
164. Mulvaney P. Surface plasmon spectroscopy of nanosized metal particles. *Langmuir.* 1996;12(3):788–800. doi:10.1021/la9502711
165. Link S, El-Sayed MA. Spectral Properties and Relaxation Dynamics of Surface Plasmon Electronic Oscillations in Gold and Silver Nanodots and Nanorods. *J Phys Chem B.* 1999;103(40):8410–8426. doi:10.1021/jp9917648
166. Liu J, Mendoza S, Roma E, Lynn MJ, Xu R, Kaifer AE. Cyclodextrin-modified gold nanospheres. Host-guest interactions at work to control colloidal properties. *J Am Chem Soc.* 1999;121(9):4304–4305.
167. Wang Y, Li H, Jin Q, Ji J. Intracellular host-guest assembly of gold nanoparticles triggered by glutathione. *Chem Commun.* 2016;52(3):582–585. doi:10.1039/c5cc07195j
168. Memişoğlu E, Bochof A, Şen M, Duchêne D, Hincal AA. Non-surfactant nanospheres of progesterone inclusion complexes with amphiphilic  $\beta$ -cyclodextrins. *Int J Pharm.* 2003;251(1–2):143–153. doi:10.1016/S0378-5173(02)00593-8
169. Da Silveira AM, Ponchel G, Puisieux F, Duchêne D. Combined poly(isobutylcyanoacrylate) and cyclodextrins nanoparticles for enhancing the encapsulation of lipophilic drugs. *Pharm Res.* 1998;15(7):1051–1055. doi:10.1023/A:1011982211632
170. Duchêne D. Cyclodextrins in targeting Application to nanoparticles. *Adv Drug Deliv Rev.* 1999;36(1):29–40. doi:10.1016/S0169-409X(98)00053-2
171. Wang Y, Han Y, Tan X, Dai Y, Xia F, Zhang X. Cyclodextrin capped gold nanoparticles (AuNP@CDs): from synthesis to applications. *J Mater Chem B.* 2021;9(11):2584–2593. doi:10.1039/d0tb02857f
172. Carofiglio T, Fornasier R, Jicsinszky L, Tonellato U, Turco C. Synthesis, characterization and chemisorption on gold of a  $\beta$ -cyclodextrin–lipoic acid conjugate. *Tetrahedron Lett.* 2001;42(31):5241–5244. doi:10.1016/S0040-4039(01)01001-2
173. Liu J, Ong W, Román E, Lynn MJ, Kaifer AE. Cyclodextrin-modified gold nanospheres. *Langmuir.* 2000;16(7):3000–3002. doi:10.1021/la991519f
174. Manickam P, Vashist A, Madhu S, et al. Gold nanocubes embedded biocompatible hybrid hydrogels for electrochemical detection of H<sub>2</sub>O<sub>2</sub>. *Bioelectrochemistry.* 2020;131:107373. doi:10.1016/j.bioelechem.2019.107373
175. Neri G, Cordaro A, Scala A, Cordaro M, Mazzaglia A, Piperno A. PEGylated bis-adamantane carboxamide as guest bridge for graphene poly-cyclodextrin gold nanoassemblies. *J Mol Struct.* 2021;1240:130519. doi:10.1016/j.molstruc.2021.130519
176. Adeli M, Sarabi RS, Yadollahi Farsi R, Mahmoudi M, Kalantari M. Polyrotaxane/gold nanoparticle hybrid nanomaterials as anticancer drug delivery systems. *J Mater Chem.* 2011;21(46):18686–18695. doi:10.1039/c1jm12412a

177. Andreani SA, Tachrim ZP, et al. The effect of  $\alpha$ -cyclodextrin and  $\beta$ -cyclodextrin as stabilizing agents on the size of gold nanoparticles. *AIP Conference Proceedings*. Vol 2493. AIP Publishing LLC; 2022:060005.
178. Shi Y, Goodisman J, Dabrowiak JC. Cyclodextrin capped gold nanoparticles as a delivery vehicle for a prodrug of cisplatin. *Inorg Chem*. 2013;52(16):9418–9426. doi:10.1021/ic400989v
179. Yang C, Wang X, Li H, Tan E, Lim CT, Li J. Cationic polyrotaxanes as gene carriers: physicochemical properties and real-time observation of DNA complexation, and gene transfection in cancer cells. *J Phys Chem B*. 2009;113(22):7903–7911. doi:10.1021/jp901302f
180. Zhang X, Zhu X, Ke F, et al. Preparation and self-assembly of amphiphilic triblock copolymers with polyrotaxane as a middle block and their application as carrier for the controlled release of Amphotericin B. *Polymer (Guildf)*. 2009;50(18):4343–4351. doi:10.1016/j.polymer.2009.07.006
181. Sierpe R, Lang E, Jara P, et al. Gold Nanoparticles Interacting with  $\beta$ -Cyclodextrin–Phenylethylamine Inclusion Complex: a Ternary System for Photothermal Drug Release. *ACS Appl Mater Interfaces*. 2015;7(28):15177–15181. doi:10.1021/acsami.5b00186
182. Park C, Youn H, Kim H, et al. Cyclodextrin-covered gold nanoparticles for targeted delivery of an anti-cancer drug. *J Mater Chem*. 2009;19(16):2310–2315. doi:10.1039/b816209c
183. Gimenez IF, Anazetti MC, Melo PS, et al. Cytotoxicity on V79 and HL60 Cell Lines by Thiolated- $\beta$ -Cyclodextrin-Au/Violacein Nanoparticles. *J Biomed Nanotechnol*. 2005;1(3):352–358. doi:10.1166/jbn.2005.041
184. Memişoğlu-Bilensoy E, Vural I, Bochoť A, et al. Tamoxifen citrate loaded amphiphilic  $\beta$ -cyclodextrin nanoparticles: in vitro characterization and cytotoxicity. *J Control Release*. 2005;104(3):489–496. doi:10.1016/j.jconrel.2005.03.006
185. Hincal AA, Memişoğlu-Bilensoy E, Bochoť A, Duchene D.  $\beta$ -cyclodextrines amphiphiles: Évaluation de nouveaux excipients pour la préparation de nanoparticules destinées à l'administration par voie parentérale ou topique. *Bull Tech Gattefossé*. 2003;96(2):59–71.
186. Zhou Y, Wang C, Wang F, Li C, Dong C, Shuang S.  $\beta$ -Cyclodextrin and its derivatives functionalized magnetic nanoparticles for targeting delivery of curcumin and cell imaging. *Chinese J Chem*. 2016;34(6):599–608. doi:10.1002/cjoc.201500756
187. Sandhu KK, McIntosh CM, Simard JM, Smith SW, Rotello VM. Gold nanoparticle-mediated transfection of mammalian cells. *Bioconjug Chem*. 2002;13(1):3–6. doi:10.1021/bc015545c
188. Wang G, Zhang J, Murray RW. DNA binding of an ethidium intercalator attached to a monolayer-protected gold cluster. *Anal Chem*. 2002;74(17):4320–4327. doi:10.1021/ac0257804
189. Fischer NO, McIntosh CM, Simard JM, Rotello VM. Inhibition of chymotrypsin through surface binding using nanoparticle-based receptors. *Proc Natl Acad Sci U S A*. 2002;99(8):5018–5023. doi:10.1073/pnas.082644099
190. Park S, Taton TA, Mirkin CA. Array-based electrical detection of DNA with nanoparticle probes. *Science*. 2002;295(5559):1503–1506.
191. Bohl Kullberg E, Bergstrand N, Carlsson J, et al. Development of EGF-conjugated liposomes for targeted delivery of boronated DNA-binding agents. *Bioconjug Chem*. 2002;13(4):737–743. doi:10.1021/bc0100713
192. Liu J, Alvarez J, Ong W, Román E, Kaifer AE. Phase transfer of hydrophilic, cyclodextrin-modified gold nanoparticles to chloroform solutions. *J Am Chem Soc*. 2001;123(45):11148–11154. doi:10.1021/ja003957a
193. Weisser M, Nelles G, Wenz G, Mittler-Neher S. Guest-host interactions with immobilized cyclodextrins. *Sensors Actuators, B Chem*. 1997;38-39(1–3):58–67. doi:10.1016/S0925-4005(97)80172-4
194. Sztandera K, Gorzkiewicz M, Klajnert-Maculewicz B. Gold nanoparticles in cancer treatment. *Mol Pharm*. 2019;16(1):1–23. doi:10.1021/acs.molpharmaceut.8b00810
195. Yao C, Zhang L, Wang J, et al. Gold nanoparticle mediated phototherapy for cancer. *J Nanomater*. 2016;5497136. doi:10.1155/2016/5497136
196. Alkilany AM, Murphy CJ. Toxicity and cellular uptake of gold nanoparticles: what we have learned so far? *J Nanoparticle Res*. 2010;12(7):2313–2333. doi:10.1007/s11051-010-9911-8
197. Hädärugá NG, Bandur GN, David I, Hädärugá DI. A review on thermal analyses of cyclodextrins and cyclodextrin complexes. *Environ Chem Lett*. 2019;17(1):349–373. doi:10.1007/s10311-018-0806-8
198. Fenyvesi É, Puskás I, Sente L. Applications of steroid drugs entrapped in cyclodextrins. *Environ Chem Lett*. 2019;17(1):375–391. doi:10.1007/s10311-018-0807-7
199. Tian B, Liu J. The classification and application of cyclodextrin polymers: a review. *New J Chem*. 2020;44(22):9137–9148. doi:10.1039/c9nj05844c
200. Heo DN, Ko W-K, Moon H-J, et al. Inhibition of osteoclast differentiation by gold nanoparticles functionalized with cyclodextrin curcumin complexes. *ACS Nano*. 2014;8(12):12049–12062.
201. Möller K, Macaulay B, Bein T. Curcumin encapsulated in crosslinked cyclodextrin nanoparticles enables immediate inhibition of cell growth and efficient killing of cancer cells. *Nanomaterials*. 2021;11(2):1–21. doi:10.3390/nano11020489
202. Lee D, Ko WK, Hwang DS, et al. Use of baicalin-conjugated gold nanoparticles for apoptotic induction of breast cancer cells. *Nanoscale Res Lett*. 2016;11(1):381. doi:10.1186/s11671-016-1586-3
203. Chen Y, Li N, Yang Y, Liu Y. A dual targeting cyclodextrin/gold nanoparticle conjugate as a scaffold for solubilization and delivery of paclitaxel. *RSC Adv*. 2015;5(12):8938–8941. doi:10.1039/c4ra13135e
204. Silva N, Riveros A, Yutronic N, et al. Photothermally controlled methotrexate release system using  $\beta$ -cyclodextrin and gold nanoparticles. *Nanomaterials*. 2018;8(12):1–15. doi:10.3390/nano8120985
205. Aykaç A, Martos-Maldonado MC, Casas-Solvas JM, et al. B-Cyclodextrin-bearing gold glyconanoparticles for the development of site specific drug delivery systems. *Langmuir*. 2014;30(1):234–242. doi:10.1021/la403454p
206. Hoshikawa A, Nagira M, Tane M, Fukushige K, Tagami T, Ozeki T. Preparation of curcumin-containing  $\alpha$ -,  $\beta$ -, and  $\gamma$ -cyclodextrin/polyethyleneglycol-conjugated gold multifunctional nanoparticles and their in vitro cytotoxic effects on A549 cells. *Biol Pharm Bull*. 2018;41(6):908–914. doi:10.1248/bpb.b18-00010
207. Hu M, Chen J, Li ZY, et al. Gold nanostructures: engineering their plasmonic properties for biomedical applications. *Chem Soc Rev*. 2006;35(11):1084–1094. doi:10.1039/b517615h
208. Norsten TB, Frankamp BL, Rotello VM. Metal directed assembly of terpyridine-functionalized gold nanoparticles. *Nano Lett*. 2002;2(12):1345–1348. doi:10.1021/nl020217m
209. Kolny J, Kornowski A, Weller H. Self-organization of cadmium sulfide and gold nanoparticles by electrostatic interaction. *Nano Lett*. 2002;2(4):361–364. doi:10.1021/nl0156843

210. Boal AK, Rotello VM. Intra-and Inter monolayer hydrogen bonding in amide-functionalized alkanethiol self-assembled monolayers on gold nanoparticles. *Langmuir*. 2000;16(24):9527–9532.
211. Si S, Mandal TK. pH-controlled reversible assembly of peptide-functionalized gold nanoparticles. *Langmuir*. 2007;23(1):190–195. doi:10.1021/la061505r
212. Li D, He Q, Cui Y, Li J. Fabrication of pH-responsive nanocomposites of gold nanoparticles/poly(4-vinylpyridine). *Chem Mater*. 2007;19(3):412–417.
213. Zhu M-Q, Wang L-Q, Exarhos GJ, Li ADQ. Thermosensitive gold nanoparticles. *J Am Chem Soc*. 2004;126(9):2656–2657. doi:10.1021/ja038544z
214. Aslan K, Luhrs CC, Pérez-Luna VH. Controlled and reversible aggregation of biotinylated gold nanoparticles with streptavidin. *J Phys Chem B*. 2004;108(40):15631–15639. doi:10.1021/jp036089n
215. Jin R, Wu G, Li Z, Mirkin CA, Schatz GC. What controls the melting properties of DNA-linked gold nanoparticle assemblies? *J Am Chem Soc*. 2003;125(6):1643–1654. doi:10.1021/ja021096v
216. Sharma J, Chhabra R, Yan H, Liu Y. pH-driven conformational switch of “i-motif” DNA for the reversible assembly of gold nanoparticles. *Chem Commun*. 2007;2(5):477–479. doi:10.1039/b612707j
217. Sudeep PK, Ipe BI, Thomas KG, et al. Fullerene-functionalized gold nanoparticles. A self-assembled Photoactive antenna-metal nanocore assembly. *Nano Lett*. 2002;2(1):29–35. doi:10.1021/nl010073w
218. Banerjee IA, Yu L, Matsui H. Application of host-guest chemistry in nanotube-based device fabrication: photochemically controlled immobilization of azobenzene nanotubes on patterned  $\alpha$ -CD monolayer/Au substrates via molecular recognition. *J Am Chem Soc*. 2003;125(32):9542–9543. doi:10.1021/ja0344011
219. Liu Z, Jiang M. Reversible aggregation of gold nanoparticles driven by inclusion complexation. *J Mater Chem*. 2007;17(40):4249–4254. doi:10.1039/b707910a
220. Liu Y, Song S-H. Cyclodextrin-modified gold nanoparticle aggregate formed by simple host-guest interactions with 1,10-phenanthroline. *J Chem Res*. 2004;3(2):152–153. doi:10.3184/030823404323000567
221. Ye BF, Zhao YJ, Cheng Y, et al. Colorimetric photonic hydrogel aptasensor for the screening of heavy metal ions. *Nanoscale*. 2012;4(19):5998–6003. doi:10.1039/c2nr31601c
222. Lyu D, Chen S, Guo W. Liposome Crosslinked Polyacrylamide/DNA Hydrogel: a Smart Controlled-Release System for Small Molecular Payloads. *Small*. 2018;14(15):1–8. doi:10.1002/sml.201704039
223. Davis ME, Pun SH, Bellocq NC, et al. Self-assembling nucleic acid delivery vehicles via linear, water-soluble, cyclodextrin-containing polymers. *Curr Med Chem*. 2004;11(2):179–197. doi:10.2174/0929867043456179
224. Costa D, Valente AJM, Miguel MG, Queiroz J. Plasmid DNA hydrogels for biomedical applications. *Adv Colloid Interface Sci*. 2014;205:257–264. doi:10.1016/j.cis.2013.08.002
225. Liu Y, Wang H, Liang P, Zhang HY. Water-soluble supramolecular fullerene assembly mediated by metallobridged  $\beta$ -cyclodextrins. *Angew Chemie Int Ed*. 2004;43(20):2690–2694. doi:10.1002/anie.200352973
226. Li F, Wang C, Guo W. Multifunctional poly-N-isopropylacrylamide/DNAzyme microgels as highly efficient and recyclable catalysts for biosensing. *Adv Funct Mater*. 2018;28(10):1–8. doi:10.1002/adfm.201705876
227. Mahalingam V, Onclin S, Péter M, Ravoo BJ, Huskens J, Reinhoudt DN. Directed self-assembly of functionalized silica nanoparticles on molecular printboards through multivalent supramolecular interactions. *Langmuir*. 2004;20(26):11756–11762. doi:10.1021/la047982w
228. Pun SH, Bellocq NC, Liu A, et al. Cyclodextrin-modified polyethylenimine polymers for gene delivery. *Bioconjug Chem*. 2004;15(4):831–840.
229. Kihara F, Arima H, Tsutsumi T, Hirayama F, Uekama K. In vitro and in vivo gene transfer by an optimized  $\alpha$ -cyclodextrin conjugate with polyamidoamine dendrimer. *Bioconjug Chem*. 2003;14(2):342–350. doi:10.1021/bc025613a
230. Forrest ML, Gabrielson N, Pack DW. Cyclodextrin-Polyethylenimine conjugates for targeted in vitro gene delivery. *Biotechnol Bioeng*. 2004;89(4):416–423. doi:10.1002/bit.20356
231. Park I-K, von Recum HA, Jiang S, Pun SH. Supramolecular assembly of cyclodextrin-based nanoparticles on solid surfaces for gene delivery. *Langmuir*. 2006;22(20):8478–8484. doi:10.1021/la061757s
232. Wang H, Chen Y, Li XY, Liu Y. Synthesis of oligo(ethylenediamino)- $\beta$ -cyclodextrin modified gold nanoparticle as a DNA concentrator. *Mol Pharm*. 2007;4(2):189–198. doi:10.1021/mp060045s
233. Qiu J, Kong L, Cao X, Li A, Tan H, Shi X. Dendrimer-entrapped gold nanoparticles modified with  $\beta$ -cyclodextrin for enhanced gene delivery applications. *RSC Adv*. 2016;6(31):25633–25640. doi:10.1039/c6ra03839e
234. Qiu J, Kong L, Cao X, et al. Enhanced delivery of therapeutic siRNA into glioblastoma cells using dendrimer-entrapped gold nanoparticles conjugated with  $\beta$ -cyclodextrin. *Nanomaterials*. 2018;8(131):1–11. doi:10.3390/nano8030131
235. Zhao D, Chen Y, Liu Y. Construction and DNA condensation of cyclodextrin-coated gold nanoparticles with anthryl grafts. *Chemistry*. 2014;9:1895–1903. doi:10.1002/asia.201402078
236. Li X, Qi Z, Liang K, et al. An artificial supramolecular nanozyme based on  $\beta$ -cyclodextrin-modified gold nanoparticles. *Catal Letters*. 2008;124(3–4):413–417. doi:10.1007/s10562-008-9494-5
237. Cao R, Villalonga R, Fragoso A. Towards nanomedicine with a supramolecular approach: a review. *IEEE Proc Nanobiotechnol*. 2005;152(5):159–164. doi:10.1049/ip-nbt
238. Villalonga R, Fragoso A, Cao R, Ortiz PD, Villalonga ML, Damiao AE. Supramolecular-mediated immobilization of trypsin on cyclodextrin-modified gold nanospheres. *Supramol Chem*. 2005;17(5):387–391. doi:10.1080/10610270500126743
239. Villalonga R, Tachibana S, Cao R, Ortiz PD, Gomez L, Asano Y. Supramolecular-mediated immobilisation of L-phenylalanine dehydrogenase on  $\beta$ -cyclodextrin-modified gold nanospheres. *J Exp Nanosci*. 2006;1(2):249–260. doi:10.1080/17458080600684487
240. Zhao Y, Huang Y, Zhu H, Zhu Q, Xia Y. Three-in-one: sensing, self-assembly, and cascade catalysis of cyclodextrin modified gold nanoparticles. *J Am Chem Soc*. 2016;138(51):16645–16654. doi:10.1021/jacs.6b07590
241. Zhou DH, Liang CC, Nie J, Zhu XQ. Construction of a repairable fixed porous catalytic bed loaded with gold nanoparticles via multivalent host-guest interactions. *ACS Sustain Chem Eng*. 2017;5(9):7587–7593. doi:10.1021/acssuschemeng.7b00879
242. An P, Xue X, Rao H, et al. Gold nanozyme as an excellent co-catalyst for enhancing the performance of a colorimetric and photothermal bioassay. *Anal Chim Acta*. 2020;1125:114–127. doi:10.1016/j.aca.2020.05.047

243. Ling XY, Reinhoudt DN, Huskens J. Reversible attachment of nanostructures at molecular printboards through supramolecular glue. *Chem Mater*. 2008;20(11):3574–3578. doi:10.1021/cm703597w
244. Ludden MJW, Reinhoudt DN, Huskens J. Molecular printboards: versatile platforms for the creation and positioning of supramolecular assemblies and materials. *Chem Soc Rev*. 2006;35(11):1122–1134. doi:10.1039/b600093m
245. Beulen MWJ, Bügler J, Lammierink B, et al. Self-assembled monolayers of heptapodant-cyclodextrins on gold. *Langmuir*. 1998;14:6424–6429.
246. Onclin S, Mulder A, Huskens J, Ravoo BJ, Reinhoudt DN. Molecular printboards: monolayers  $\beta$ -cyclodextrins on silicon oxide surfaces. *Langmuir*. 2004;20(13):5460–5466. doi:10.1021/la049561k
247. Huskens J, Deij MA, Reinhoudt DN. Attachment of molecules at a molecular printboard by multiple host-guest interactions. *Angew Chemie Int Ed*. 2002;41(23):4467–4471. doi:10.1002/1521-3773(20021202)41:23<4467::AID-ANIE4467>3.0.CO;2-M
248. Crespo-Biel O, Dordí B, Reinhoudt DN, Huskens J. Supramolecular layer-by-layer assembly: alternating adsorptions of guest- and host-functionalized molecules and particles using multivalent supramolecular interactions. *J Am Chem Soc*. 2005;127(20):7594–7600. doi:10.1021/ja051093t
249. Crespo-Biel O, Jukovic A, Karlsson M, Reinhoudt DN, Huskens J. Multivalent aggregation of cyclodextrin gold nanoparticles and adamantyl-terminated guest molecules. *Isr J Chem*. 2005;45(3):353–362. doi:10.1560/af3p-k2a6-mdck-1678
250. Maury P, Crespo-Biel O, Péter M, Reinhoudt DN, Huskens J. Integration of top-down and bottom-up nanofabrication schemes. *Mater Res Soc Symp Proc*. 2005;901:441–449. doi:10.1557/proc-0901-rb12-01
251. Ling XY, Phang IY, Reinhoudt DN, Vancso GJ, Huskens J. Supramolecular layer-by-layer assembly of 3D multicomponent nanostructures via multivalent molecular recognition. *Int J Mol Sci*. 2008;9(4):486–497. doi:10.3390/ijms9040486
252. Crespo-Biel O, Péter M, Bruinink CM, Ravoo BJ, Reinhoudt DN, Huskens J. Multivalent host-guest interactions between  $\beta$ -cyclodextrin self-assembled monolayers and poly(isobutene-alt-maleic acid)s modified with hydrophobic guest moieties. *Chem - a Eur J*. 2005;11(8):2426–2432. doi:10.1002/chem.200400393
253. Zuo F, Luo C, Zheng Z, Ding X, Peng Y. Supramolecular assembly of  $\beta$ -cyclodextrin-capped gold nanoparticles on ferrocene-functionalized ITO surface for enhanced voltammetric analysis of ascorbic acid. *Electroanalysis*. 2008;20(8):894–899. doi:10.1002/elan.200704113
254. Gómez-Graña S, Pérez-Juste J, Hervés P. Cyclodextrins and inorganic nanoparticles: another tale of synergy. *Adv Colloid Interface Sci*. 2021;288:102338. doi:10.1016/j.cis.2020.102338
255. Yun Y. Electrochemical sensor for ultrasensitive determination of bisphenol a based on gold nanoparticles/ $\beta$ -cyclodextrin functionalized reduced graphene oxide nanocomposite. *Int J Electrochem Sci*. 2016;11(4):2778–2789. doi:10.20964/110402778
256. Wu H, Fang F, Wang C, Hong X, Chen D, Huang X. Selective molecular recognition of low density lipoprotein based on  $\beta$ -cyclodextrin coated electrochemical biosensor. *Biosensors*. 2021;11(7):1–10. doi:10.3390/bios11070216
257. Chen M, Diao G. Electrochemical study of mono-6-thio- $\beta$ -cyclodextrin/ferrocene capped on gold nanoparticles: characterization and application to the design of glucose amperometric biosensor. *Talanta*. 2009;80(2):815–820. doi:10.1016/j.talanta.2009.07.068
258. Díez P, Piuleac CG, Martínez-Ruiz P, et al. Supramolecular immobilization of glucose oxidase on gold coated with cyclodextrin-modified cysteamine core PAMAM G-4 dendron/Pt nanoparticles for mediatorless biosensor design. *Anal Bioanal Chem*. 2013;405(11):3773–3781. doi:10.1007/s00216-012-6491-8
259. Zheng X, Li L, Cui K, et al. Ultrasensitive enzyme-free biosensor by coupling cyclodextrin functionalized Au nanoparticles and high-performance Au-paper electrode. *ACS Appl Mater Interfaces*. 2018;10(4):3333–3340. doi:10.1021/acsami.7b17037
260. Zhang NMY, Qi M, Wang Z, et al. One-step synthesis of cyclodextrin-capped gold nanoparticles for ultra-sensitive and highly-integrated plasmonic biosensors. *Sensors Actuators, B Chem*. 2019;286:429–436. doi:10.1016/j.snb.2019.01.166
261. Luo S, Wu Y, Mou Q, Li J, Luo X. A thio- $\beta$ -cyclodextrin functionalized graphene/gold nanoparticle electrochemical sensor: a study of the size effect of the gold nanoparticles and the determination of tetrabromobisphenol A. *RSC Adv*. 2019;9(31):17897–17904. doi:10.1039/c9ra02614b
262. Rajamanikandan R, Lakshmi AD, Ilanchelian M. Smart phone assisted, rapid, simplistic, straightforward and sensitive biosensing of cysteine over other essential amino acids by  $\beta$ -cyclodextrin functionalized gold nanoparticles as a colorimetric probe. *New J Chem*. 2020;44(28):12169–12177. doi:10.1039/d0nj02152k
263. Kapan B, Kurbanoglu S, Esenturk EN, Soylemez S, Toppare L. Electrochemical catechol biosensor based on  $\beta$ -cyclodextrin capped gold nanoparticles and inhibition effect of ibuprofen. *Process Biochem*. 2021;108:(June):80–89. doi:10.1016/j.procbio.2021.06.004
264. Fang A, Feng D, Luo X, Shi F. Gold nanoparticles prepared with cyclodextrin applied to rapid vertical flow technology for the detection of Brucellosis. *Biosensors*. 2022;12(7):75. doi:10.3390/bios12070531
265. Peng L, You M, Wu C, et al. Reversible phase transfer of nanoparticles based on photoswitchable host-guest chemistry. *ACS Nano*. 2014;8(3):2555–2561. doi:10.1021/nn4061385
266. Tokuyama H, Yamago S, Nakamura E, Shiraki T, Sugiura Y. Photoinduced biochemical activity of fullerene carboxylic acid. *J Am Chem Soc*. 1993;115(17):7918–7919. doi:10.1021/ja00070a064
267. Liu Y, Zhao YL, Chen Y, Liang P, Li L. A water-soluble  $\beta$ -cyclodextrin derivative possessing a fullerene tether as an efficient photodriven DNA-cleavage reagent. *Tetrahedron Lett*. 2005;46(14):2507–2511. doi:10.1016/j.tetlet.2005.01.181
268. Xie SY, Bin HR, Yu LJ, Ding J, Zheng LS. Microwave synthesis of fullerenes from chloroform. *Appl Phys Lett*. 1999;75(18):2764–2766. doi:10.1063/1.125142
269. Murthy CN, Geckeler KE. The water-soluble  $\beta$ -cyclodextrin-[60]fullerene complex. *Chem Commun*. 2001;1(13):1194–1195. doi:10.1039/b102142g
270. Liu Y, Yang YW, Chen Y. Thio[2-(benzoylamino)ethylamino]- $\beta$ -CD fragment modified gold nanoparticles as recycling extractors for [60] fullerene. *Chem Commun*. 2005;2(33):4208–4210. doi:10.1039/b507650a
271. Liu J, Alvarez J, Ong W, Kaifer AE. Network aggregates formed by C60 and gold nanoparticles capped with  $\gamma$ -cyclodextrin hosts. *Nano Lett*. 2001;1(2):57–60. doi:10.1021/nl0001813
272. Liu Y, Yang YW, Chen Y, Zou HX. Polyrotaxane with cyclodextrins as stoppers and its assembly behavior. *Macromolecules*. 2005;38(13):5838–5840. doi:10.1021/ma047327v
273. Liu Y, Wang H, Chen Y, Ke CF, Liu M. Supramolecular aggregates constructed from gold nanoparticles and L-Try-CD polypseudorotaxanes as captors for fullerenes. *J Am Chem Soc*. 2005;127(2):657–666. doi:10.1021/ja046294w

International Journal of Nanomedicine

Dovepress

### Publish your work in this journal

The International Journal of Nanomedicine is an international, peer-reviewed journal focusing on the application of nanotechnology in diagnostics, therapeutics, and drug delivery systems throughout the biomedical field. This journal is indexed on PubMed Central, MedLine, CAS, SciSearch<sup>®</sup>, Current Contents<sup>®</sup>/Clinical Medicine, Journal Citation Reports/Science Edition, EMBase, Scopus and the Elsevier Bibliographic databases. The manuscript management system is completely online and includes a very quick and fair peer-review system, which is all easy to use. Visit <http://www.dovepress.com/testimonials.php> to read real quotes from published authors.

Submit your manuscript here: <https://www.dovepress.com/international-journal-of-nanomedicine-journal>